2021

Therapeutic Immunoglobulin G Surface Mobility Promotes Antibody-Dependent Cellular Phagocytosis by Arp2/3 and Syk Mediated Rearrangement of Fcγ Receptors

Seongwan Jo
South Dakota State University

THERAPUTIC IMMUNOGLOBULIN G SURFACE MOBILITY PROMOTES ANTIBODY-DEPENDENT CELLULAR PHAGOCYTOSIS BY ARP2/3 AND SYK MEDIATED REARRANGEMENT OF FCγ RECEPTORS

BY

SEONGWAN JO

A thesis submitted in partial fulfillment of the requirements for the

Master of Science

Major in Biochemistry

South Dakota State University

2021

THESIS ACCEPTANCE PAGE

Seongwan Jo

This thesis is approved as a creditable and independent investigation by a candidate for the master's degree and is acceptable for meeting the thesis requirements for this degree. Acceptance of this does not imply that the conclusions reached by the candidate are necessarily the conclusions of the major department.

Adam Hoppe
Advisor Date

Douglas Raynie
Department Head Date

Nicole Lounsbery, PhD
Director, Graduate School Date

ACKNOWLEDGEMENTS

I would like to express my deep and sincere gratitude to my advisor, Dr. Adam Hoppe for giving me the opportunity to do research and providing invaluable guidance. His immense knowledge, motivation, enthusiasm, and patience inspired me. He has taught me the methodology and knowledge to carry out the research and to present research findings. It was a great privilege to work under his guidance. I am extremely grateful for what he has offered me. I would also like to thank him for his friendship, empathy, and great sense of humor. I am extending my heartfelt thanks to his wife, Dr. Natalie Thiex, who also supported me throughout my study.

I thank my fellow labmates: Jason Kerkvilet, Sadam Hossain, and Seuly Akter for the stimulating discussions and for all the fun we have had. Also, I thank my friends Nicholas Cronin and Dr. Brandon Scott for enlightening me the first glance of research when I was an undergraduate and for helping me finish up my research project.

Much appreciation goes to my sister, Eunhee Kang, and her husband, Jimmy Kang, who motivated me to be a better individual and all the support during my study. Lastly, my parents, Jinhaeng Jo and Misun Park, I appreciate for giving me an opportunity of studying in US and for your guidance to become an independent individual.

CONTENTS

LIST OF FIGURES

ABSTRACT

THERAPUTIC IMMUNOGLOBULIN G SURFACE MOBILITY PROMOTES ANTIBODY-DEPENDENT CELLULAR PHAGOCYTOSIS BY ARP2/3 AND SYK MEDIATED REARRANGEMENT OF FCγ RECEPTORS

SEONGWAN JO

2021

Therapeutic antibodies are rapidly growing class of drugs for treating cancers and immunological disorders by targeting specific antigens or blocking certain pathway to inhibit the tumor growth. In cancer immunotherapy, it was found that Fcγ receptor (FcγR) in immune cells play an important role in antibody dependent cell toxicity against tumor cells. Therefore, understanding FcγR activation mechanism, which requires ligation with immunoglobulin (IgG), is crucial to enhance potency of therapeutic antibodies. One crucial immune responses triggered upon FcγR ligation with IgG is phagocytosis which indicates clearing targets by engulfment. It is known that FcγRs form microclusters which gets rearranged during engagement (J. Lin et al., 2016). Receptor microclustering is important for other immune receptors such as B cell receptor (BCR) and T cell receptor (TCR) (Bolger-Munro et al., 2019; Hashimoto-Tane & Saito, 2016). However, the implications of FcγR rearrangement for antibody-based therapies and cellular effector mechanisms has not been studied. This thesis, examined the dynamics of IgG microclustering and recruitment of Syk kinase to microclusters during antibody dependent cellular phagocytosis (ADCP) using confocal and lattice light sheet (LLS) imaging. Additionally, Total Internal Reflection Fluorescence (TIRF) imaging was used

to image the organization of IgG and Syk microclusters during engagement on IgG opsonized supported lipid bilayers (SLBs). The major findings is that surface mobility of the IgG/FcγR complexes enhances ADCP. Moreover, proper Syk and Arp2/3 activity is required for organizing IgG/FcγR complexes during target engulfment and suppressing trogocytic clearance of IgG from the target cell. Together, this study uncovers an important role of antibody mobility in contributing to effective ADCP of target cells.

CHAPTER 1: INTRODUCTION

Introduction

Immune receptors such as FcγR, BCR, and TCR are important for innate and adaptive immune responses. For activating immune responses, immune receptors are stimulated by multivalent ligands instead of the conformational changes (Holowka, Sil, Torigoe, & Baird, 2007; Jaumouille et al., 2014; Woof & Burton, 2004). Upon clustering of immune receptors, phosphorylation of immunoreceptor tyrosine based activating motifs (ITAM), found in their cytoplasmic tails or associated adaptors by Src-family kinases, initiates signal transduction. Immune receptors also possess immunoreceptor tyrosine based inhibitory motif (ITIM) which, when phosphorylated, suppresses immune receptor signaling by recruiting the phosphatidylinositol phosphatases SHIP-1/2 (Nimmerjahn & Ravetch, 2008). The effective balancing of activating and inhibitory signaling is required to properly trigger immune responses such as phagocytosis. Therefore, understanding the FcγR clustering event is important for understanding the regulation of immunoreceptor signaling.

Previous studies suggested a key role of actin cytoskeleton for regulating immunoreceptor clustering by manipulating the collision rate among immune receptors via changing the mobility of immune receptors (Jaumouille et al., 2014; Liu et al., 2013; Rey-Suarez et al., 2020). Therefore, understanding the mechanism of actin regulation is also crucial to study FcγR clustering. FcγR signaling can also stimulate actin branching which suggests that FcγR and actin are dependent on each other(Swanson & Hoppe, 2004). Our lab recently found that the mobility of antigen-antibody complexes can affect

FcγR signaling. Together, manipulation of FcγR mediated activating and inhibitory signaling can be achieved by understanding different factors that can affect FcγR clustering. Thorough understanding of FcγR clustering and actin regulatory mechanisms is required to understand the mechanism of ADCP.

The FcγR family

FcγRs have multifaceted roles in the immune system. The knowledge related to FcγRs could be translated into treating diseases using therapeutic antibodies. FcγRs have been primarily studied in mice and in humans. They are similar in both species, but

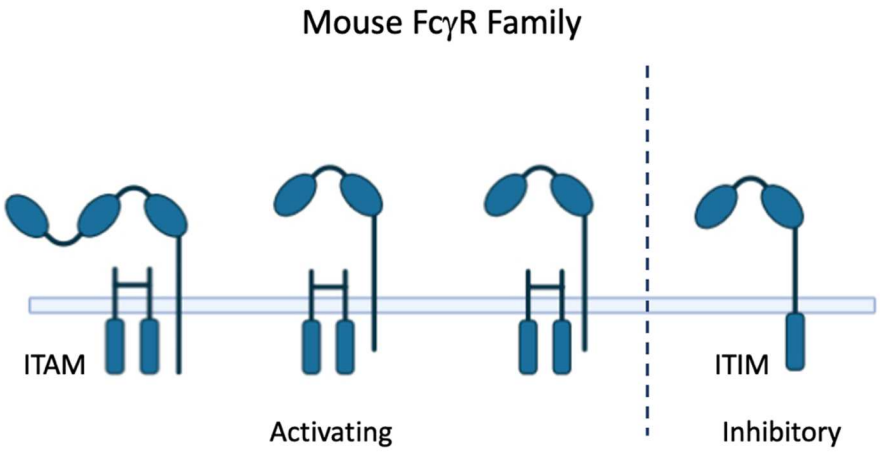

Name	FcγRI	FcγRIII	FcγRIV	FcγRIIb
Affinity	High	Low - Medium	Low - Medium	Low - Medium
Specificity	IgG2a, IgG2b	IgG1, IgG2a, IgG2b	IgG2a, IgG2b	IgG1, IgG2a, IgG2b

Figure 1.1 The mouse FcγR Family. A) There are activating and inhibitory receptors among in the mouse FcγR family with varying affinity and specificity to different IgGs. FcγRI has the high affinity while others have low to medium affinity (Created with BioRender.com)

human FcγR systems are more complex than the mouse FcγR system (Nimmerjahn, 2008, Nimmerjahn, 2006). However, many of the fundamental principles and cellular mechanisms found from mice have been enumerated in humans. Here we will focus on the murine FcγRs.

There are four different FcγRs in the mouse FcγR family (Fig 1.1) which corresponds to other mammalian species including human and primates (Nimmerjahn, 2006). The mouse FcγR family consists of three activating receptors and one inhibitory receptor (Fig 1.1). The overall structure of FcγR family contains an extracellular portion binding to ligands and γ-chain dimer containing ITAM and ITIM. The low-affinity receptors have two extracellular Immunoglobulin (Ig)-like domains, whereas the high-affinity receptor FcγRI contains three Ig-like domains. FcγRI is the most studied high affinity receptor which binds to IgG2a with an affinity of 10^8-10^9 M^{-1}; All other FcγRs have a 100-1000 fold lower affinity to a broader IgG subclass specificity (Nimmerjahn, 2008). For instance, IgG1, IgG2a and IgG2b can bind to mouse FcγRIIB and FcγRIII with lower affinity. The transmembrane region of FcγRs contains FcRγ chain (FcRγ) that is associated via salt bridges between the basic amino acids on the receptor and acidic residues of the γ-chain dimer (Brandsma, Hogarth, Nimmerjahn, & Leusen, 2016). The activating receptors, FcγRI, FcγRIII and FcγRIV, have ITAM within an associated dimer. Whereas the inhibitory receptor, FcγRIIB, contains ITIM on the cytoplasmic tail. Upon ligation, FcγR signaling can be transduced via ITAM and ITIM which is required for phagocytosis.

ITAM and ITIM signaling

Immune receptor signaling involves complex intracellular signaling upon binding to opsonized targets. One of the most important phenomena for immune receptor signaling activation is often referred as clustering. Clustering is a common trait of immune receptors such as TCR, BCR, and FcRs. Both TCRs and BCRs cluster at the central super molecular activation complex (cSMAC) in the immunological synapse

(Grakoui et al., 1999; K. B. Lin et al., 2008). FcγRs also form clusters upon ligation with IgG on the opsonized targets (J. Lin et al., 2016; Sobota et al., 2005). The clustering of TCR, BCR and FcγRs trigger phosphorylation of ITAM's tyrosine by Src Family Kinase such as Lyn (Goodridge et al., 2011; Grakoui et al., 1999; K. B. Lin et al., 2008). The phosphorylation of ITAMs leads to recruitment of Syk in BCRs and FcγRs, and Zap 70 in TCRs via binding of two Src homology 2 (SH2) domains and to phosphorylated ITAM's tyrosine (Mocsai, Ruland, & Tybulewicz, 2010). After binding, Syk and Zap 70 are activated which amplify immunoreceptor signaling to drive downstream immune responses such as antibody secretion, cytotoxity and phagocytosis mediated by BCR, TCR and FcγR signaling (Frank et al., 2004; X. Li & Kimberly, 2014; Lowell, 2011; Mocsai et al., 2010).

Inhibitory signaling is also required to trigger effective immune responses. The inhibitory FcγRIIb can cluster with activated TCRs, BCRs and FcγRs which causes the phosphorylation of ITIM's tyrosines (X. Li & Kimberly, 2014; Stanford, Rapini, & Bottini, 2012). Then, SH2 domain containing phosphatases such as SHIP and SHP-1 are recruited to Tyrosine-phosphorylated ITIM. SHIP can catalyze dephosphorylation of phosphatidylinositol-3,4,5-trisphosphate (PIP_3) to phosphatidylinositol-4,5-bisphosphate (PIP_2), while SHP-1 act as phosphatase of pTyr. In turn, the activating ITAM signaling is inhibited. ITAM and ITIM signals balance the overall immune responses activated by immune receptors.

FcγR mediated antibody dependent cellular phagocytosis

Macrophages, monocytes and dendritic cells express FcγRs to varying degrees and are resident in nearly all tissues of the body making them key effectors of IgG-mediated responses and antigen presentation (Barkal et al., 2018; Dahal et al., 2017; Gordan, Biburger, & Nimmerjahn, 2015; Gordon et al., 2017; Shapouri-Moghaddam et al., 2018; Weiskopf & Weissman, 2015). When FcγR signal activation dominates the

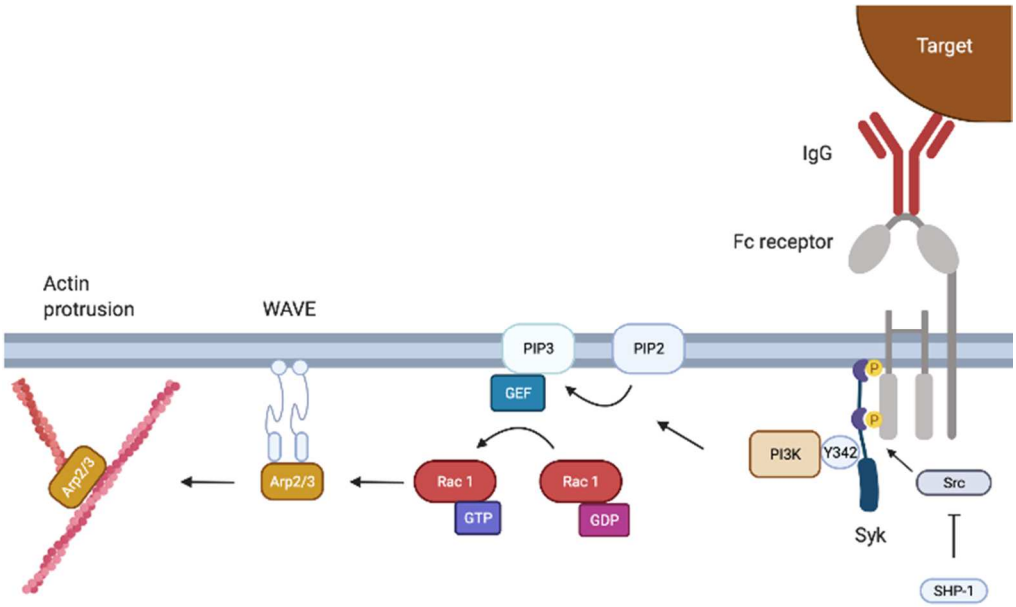

Figure 1.2 The FcγR Signaling. A) Binding between activating FcγRs and IgG on the phagocytic targets activates FcγR signaling. Syk is activated by binding to ITAM phosphorylated by Src. Then, PI3K bound to tyrosine 342 of Syk converts PIP2 to PIP3 which activates Rac1 activity. At the end, Arp2/3 binds to WASP which can then be used for actin branching and polymerization. This whole process can also be inhibited by inhibitory signal such as SHP-1 (Created with BioRender.com).

cellular system, it can trigger multiple immune responses including cytokine secretion, antibody-dependent cell-mediated cytotoxicity (ADCC) and ADCP. In macrophages, ADCP is initiated via binding between activating FcγRs and IgG on the phagocytic targets (Fig 1.2). Clustering of activating FcγRs induce phosphorylation of ITAM's tyrosines by Src-family kinases which triggers Syk recruitment and binding via

tandem SH2 domain to ITAM (X. Li & Kimberly, 2014; Lowell, 2011; Mocsai et al., 2010). Phosphoinositide 3-kinase (PI3K) is then recruited to activated Syk by interaction between p85 on PI3K and phosphorylated Tyr342 on Syk. This interaction induces the conversion from PIP_2 to PIP_3. After conversion, PIP_3 can be act as a docking site for PH domain containing proteins such as VAV which is a Rac GEF. Vav can activate Rac1 by catalyzing the conversion of Rac1 GDP to Rac1 GTP. Activated Rac1 induce Arp2/3 binding to WAVE which stimulates actin branching and polymerization which triggers ADCP that fully engulf the opsonized phagocytic target. This complicated process can be inhibited by phosphatases including SHP-1 is thought to antagonize the Syk/PI3K signaling by dephosphorylation (Abram & Lowell, 2017). Such dephosphorylation can inhibit ADCP. Together, combining activating and inhibitory mechanisms of FcγR signaling induce effective ADCP by controlling actin branching and nucleation.

Regulation of actin cytoskeleton in phagocytosis

The cytoskeleton is a filament network in the cytoplasm of eukaryotic cells that is critical for maintaining the cell shape, locomotion of the cell, transporting proteins in the cell body and movement of organelles (Fletcher & Mullins, 2010). Cytoskeletal polymer is mainly comprised of actin filaments, microtubules and intermediate filaments. These polymers work together to control the shape and maintain the integrity of intracellular compartments (Fletcher & Mullins, 2010)

The actin cytoskeleton plays an important role including cell motility, morphology and immune responses. Therefore, understanding actin dynamics and polymerization is crucial. Actin is a globular protein that is essentially found in most eukaryotic cells which forms actin filament (Dominguez & Holmes, 2011). Actin is

involved in a variety of cellular mechanisms thanks to its ability to transition between monomeric (G-actin) and filamentous (F-actin) states. With G-actin being the actin subunit for F-actin, actin filament has fast growing (barbed) and slow growing (pointed) ends. Actin polymerization is an active energy-consuming process. Actin monomers have affinity to ATP which provides the energy for the actin polymerization; ATP-actin monomers are favored to be added at the barbed ends, while ADP-actin monomers are lost from pointed ends (Millard, Sharp, & Machesky, 2004). This process forms a right-handed, two-chained long helix structure which have 13 G-actins per turn with -166.6±0.6˚ and the rise per molecule being 2.76 nm (Dominguez & Holmes, 2011; Watrach, Hanson, & Watrach, 1963). Combining with such structure, actin filament grows toward the cell membrane which promotes actin protrusion (Millard et al., 2004). Therefore, actin filament is one of the most important components of phagocytosis. Previous studies confirmed that actin's role is tightly regulated by actin-related proteins 2/3 (Arp2/3) complex which is a key regulator of actin nucleation and branching (Frank et al., 2004; Pollard & Borisy, 2003; Pollitt & Insall, 2009). However, Arp2/3 complex is not sufficient to initiate actin polymerization on its own (Machesky et al., 1999). Arp2/3 complex requires support from members of Wiskott-Aldrich syndrome protein (WASP) family and suppressor of the cAMP receptor (SCAR)/WASP-family verprolin homologous protein (WAVE) (Millard et al., 2004; Pollitt & Insall, 2009). Specifically, WAVE is involved in linking signaling pathway to regulate the actin cytoskeleton. Moreover, the balancing between actin assembly and disassembly is crucial for phagocytosis. As the cell only has limited resources, actin monomer disassembly is required to add actin monomers to the growing end of actin filament. There are several

proteins known for actin disassembly such as Gelsolin and actin-depolymerizing factor (ADF)/cofilin (Dominguez & Holmes, 2011; Kotila et al., 2019). Gelsolin requires binding to Ca^{2+} which exposes actin binding sites and sever actin filaments (Burtnick et al., 1997; Dominguez & Holmes, 2011; Kotila et al., 2019). ADF/cofilin catalyzes actin filament severing and depolymerization (Dominguez & Holmes, 2011). ADF/cofilin works together with cyclase-associated-protein (CAP) to depolymerize actin filaments more rapidly (Kotila et al., 2019). However, there is significantly less knowledge established on actin disassembly compare to actin nucleation, polymerization and capping.

WASP family

The WASP family protein classes include WASH, WASP and WAVE. WASP and WAVE will be discussed as they are the most studied WASP family proteins. WASPs are named after Wiskott-Aldrich syndrome (Pollitt & Insall, 2009). Whereas SCAR/WAVE have two different names as they were discovered by two groups although WAVE is more commonly used on mammalian cells (Millard et al., 2004; Pollitt & Insall, 2009). WASP family proteins are important nucleation promoting factors (NPFs) as they play an important role for *de novo* actin nucleation and polymerization by interaction with the Arp2/3 complex (Millard et al., 2004; Pollitt & Insall, 2009; Takenawa & Suetsugu, 2007).

Regulation of WASP family depends on domains in N-terminus which interact with PIP_2 and the Rho-family GTPases including Cdc 42 and Rac (Kotila et al., 2019; Millard et al., 2004; Pollitt & Insall, 2009). C-terminal of WASP has verprolin-homolgy, cofilin-homology, acidic (VCA) domain which can directly bind and activate Arp2/3,

however, WASP is predominantly in an autoinhibited conformation which occlude VCA domain (Eden, Rohatgi, Podtelejnikov, Mann, & Kirschner, 2002). Binding between WASP homology 1 (WH1) domain in N-terminus of WASP and the small GTPase Cdc42 can activate WASP by changing conformation to expose VCA domain (Eden et al., 2002; Kim, Kakalis, Abdul-Manan, Liu, & Rosen, 2000). Whereas interaction between WH1 domain and WASP-interacting protein (WIP) family of proteins suppresses the WASP activity (Kim et al., 2000; Pollitt & Insall, 2009). Similar to WASP, SCAR/WAVE also has C-terminal VCA domain, but it is not autoinhibited and does not contain WH1 domain. SCAR/WAVE1 form part of the WAVE1 regulatory complex (WRC) which include Sra1, Nap1, Abi and HSPC300 genes (B. Chen et al., 2017; Eden et al., 2002; Pollitt & Insall, 2009; Takenawa & Suetsugu, 2007). Macrophages primarily express WAVE2 coding genes including WASF2, Nckap1L, Abi1, Brk and Cyfip1 (Kheir, Gevrey, Yamaguchi, Isaac, & Cox, 2005; Park, Chan, & Iritani, 2010). SCAR/WAVE is inhibited in WRC, however, the interaction between Sra1 and the small GTPase Rac activates WAVE function by exposing VCA domain (B. Chen et al., 2017). Moreover, both WASP and SCAR/WAVE contain basic domain that interact with PIP_2 which also activate WASP and SCAR/WAVE to interact with Arp2/3 (Pollitt & Insall, 2009).

The Arp2/3 complex

The Arp2/3 complex has seven subunits comprised of Arp2, Arp3 and Arp2/3 complex (ARPC) ARPC1 - ARPC5 (Goley et al., 2010; Pollitt & Insall, 2009; Rotty, Wu, & Bear, 2013). Arp2 and Arp3 are tightly related to monomeric actin polymerization, while ARPC 1-5 are important for binding to F-actin and localization of Arp2/3 complex (Goley et al., 2010; Rotty et al., 2013). As mentioned above, WASP family proteins

interact with the Arp2/3 complex to catalyze actin nucleation and polymerization. The activated Arp2/3 complex works together with formins for actin polymerization which is not spontaneous due to a high kinetic barrier. Formins elongate single actin filaments, while the Arp2/3 complex nucleates new actin monomers at a 70˚ angle from the side of pre-existing filaments (Breitsprecher & Goode, 2013; Millard et al., 2004; Pollitt & Insall, 2009). Historically, there are two proposed models on the Arp2/3 complex mechanism during actin nucleation – the side branching model and the barbed-end branching model (Egile et al., 2005; Millard et al., 2004; Mullins, Heuser, & Pollard, 1998; Pantaloni, Boujemaa, Didry, Gounon, & Carlier, 2000). The side branching model suggests that a new actin filament branch grow from the branch junction formed by Arp2/3 complex on the side of an existing filament; Therefore, the actin nucleation rate depends on the length of an existing actin filament (Egile et al., 2005; Millard et al., 2004). Although the side branching model is more popular, the barbed-end branching model is also proposed as an alternative model. The barbed-end branching model suggests that the barbed end of the actin filament is where the activated Arp2/3 complex binds rather than the side of an existing actin filament; Therefore, the actin nucleation rate depends on the available barbed ends (Millard et al., 2004; Pantaloni et al., 2000). This process allows cells to form the integrated actin networks that is essential in eukaryotic cells. Thus, the Arp2/3 complex is extremely important for many cellular processes such as endocytosis, phagocytosis, vesicle motility, migration and adhesion (Goley et al., 2010; Millard et al., 2004).

Regulation of immune receptor microclustering by actin cytoskeleton

Microclustering of immune receptors appears to be central to their function and is likely governed by actin polymerization. There are evidences that actin plays a key role in regulating immune receptor microclustering. For example, BCR mobility is significantly decreased after constitutive loss or acute inhibition of the WASP which resulted in lack of signal down-regulation (Liu et al., 2013; Rey-Suarez et al., 2020). Without WASP, the actin dynamics of B cell was reduced during engagement on BCR specific antibody coated surface. The reduced actin dynamics suppressed the diffusivity of a stimulatory co-receptor, CD19, whereas the effect on diffusivity of inhibitory receptor, FcγRIIB, was limited; This could result in lack of mixing with FcγRIIB with BCR and constant activation signaling (Liu et al., 2013). Also, FcγR lateral mobility and clustering are regulated by Syk mediated actin cytoskeleton reorganization. The transmembrane proteins bound directly to actin cytoskeleton such as CD44 can form barriers around FcγR which suppress FcγR mobility (Freeman et al., 2018). However, Syk signal stimulate organizing actin meshwork which influences FcγR mobility and signals (Jaumouille et al., 2014). These studies suggest the actin's role on immune receptor mobility and signaling, therefore, the importance of Arp2/3 and WASP family proteins on regulating immune responses. However, more study is needed to elucidate the mechanism of actin activity during immune responses.

The effect of antigen-antibody mobility on ADCP

The antibody mobility on the target surface could also affect immune receptor mobility. There are studies suggesting the importance of ligand mobility for TCR and BCR signaling. The high ligand mobility enhanced TCR and BCR activation compared to low ligand mobility (Hsu et al., 2012; Ketchum, Miller, Song, & Upadhyaya, 2014).

However, the effect of antigen-antibody mobility on FcγR signaling is not studied at all. To conduct this research, we manipulated the mobility of antigen-antibody on Wil2s cells and supported lipid bilayers (SLBs). Different drug treatment was used on Wil2s cell, while lipid compositions were used for SLBs to manipulate the antigen-antibody mobility. This thesis will provide the new insight of antibody mobility on the target surface affecting phagocytic response by changing the degree of FcγR microclustering. Also, the importance of Syk reorganization for successful phagocytosis and suppress trogocytosis by regulating actin dynamics will be discussed.

References

Ackerman, M. E., Dugast, A. S., McAndrew, E. G., Tsoukas, S., Licht, A. F., Irvine, D. J., & Alter, G. (2013). Enhanced phagocytic activity of HIV-specific antibodies correlates with natural production of immunoglobulins with skewed affinity for FcgammaR2a and FcgammaR2b. *J Virol, 87*(10), 5468-5476. doi:10.1128/JVI.03403-12

Alvey, C., & Discher, D. E. (2017). Engineering macrophages to eat cancer: from "marker of self" CD47 and phagocytosis to differentiation. *J Leukoc Biol, 102*(1), 31-40. doi:10.1189/jlb.4RI1216-516R

Alvey, C. M., Spinler, K. R., Irianto, J., Pfeifer, C. R., Hayes, B., Xia, Y., . . . Discher, D. E. (2017). SIRPA-Inhibited, Marrow-Derived Macrophages Engorge, Accumulate, and Differentiate in Antibody-Targeted Regression of Solid Tumors. *Curr Biol, 27*(14), 2065-2077 e2066. doi:10.1016/j.cub.2017.06.005

Bailey, E. M., Choudhury, A., Vuppula, H., Ortiz, D., Schaeck, J., Manning, A. M., . . . Hoppe, A. D. (2020). Engineered IgG1-Fc molecules define valency control of cell surface Fcg receptor inhibition and activation in endosomes. doi:10.3389/fimmu.2020.617767

Bakalar, M. H., Joffe, A. M., Schmid, E. M., Son, S., Podolski, M., & Fletcher, D. A. (2018). Size-Dependent Segregation Controls Macrophage Phagocytosis of Antibody-Opsonized Targets. *Cell, 174*(1), 131-142 e113. doi:10.1016/j.cell.2018.05.059

Barkal, A. A., Weiskopf, K., Kao, K. S., Gordon, S. R., Rosental, B., Yiu, Y. Y., . . . Maute, R. L. (2018). Engagement of MHC class I by the inhibitory receptor LILRB1 suppresses macrophages and is a target of cancer immunotherapy. *Nat Immunol, 19*(1), 76-84. doi:10.1038/s41590-017-0004-z

Boudreau, C. M., & Alter, G. (2019). Extra-Neutralizing FcR-Mediated Antibody Functions for a Universal Influenza Vaccine. *Front Immunol, 10*, 440. doi:10.3389/fimmu.2019.00440

Brandsma, A. M., Schwartz, S. L., Wester, M. J., Valley, C. C., Blezer, G. L. A., Vidarsson, G., . . . Leusen, J. H. W. (2018). Mechanisms of inside-out signaling of the high-affinity IgG receptor FcgammaRI. *Sci Signal, 11*(540). doi:10.1126/scisignal.aaq0891

Breitsprecher, D., & Goode, B. L. (2013). Formins at a glance. *J Cell Sci, 126*(Pt 1), 1-7. doi:10.1242/jcs.107250

Burtnick, L. D., Koepf, E. K., Grimes, J., Jones, E. Y., Stuart, D. I., McLaughlin, P. J., & Robinson, R. C. (1997). The crystal structure of plasma gelsolin: implications for actin severing, capping, and nucleation. *Cell, 90*(4), 661-670. doi:10.1016/s0092-8674(00)80527-9

Chao, M. P., Alizadeh, A. A., Tang, C., Myklebust, J. H., Varghese, B., Gill, S., . . . Majeti, R. (2010). Anti-CD47 antibody synergizes with rituximab to promote phagocytosis and eradicate non-Hodgkin lymphoma. *Cell, 142*(5), 699-713. doi:10.1016/j.cell.2010.07.044

Chen, B., Chou, H. T., Brautigam, C. A., Xing, W., Yang, S., Henry, L., . . . Rosen, M. K. (2017). Rac1 GTPase activates the WAVE regulatory complex through two distinct binding sites. *Elife, 6*. doi:10.7554/eLife.29795

Chertkova, A. O., Mastop, M., Postma, M., van Bommel, N., van der Niet, S., Batenburg, K. L., . . . Goedhart, J. (2020). Robust and Bright Genetically Encoded Fluorescent Markers for Highlighting Structures and Compartments in Mammalian Cells. *BioRxiv*, 160374. doi:10.1101/160374

Church, A. K., VanDerMeid, K. R., Baig, N. A., Baran, A. M., Witzig, T. E., Nowakowski, G. S., & Zent, C. S. (2016). Anti-CD20 monoclonal antibody-dependent phagocytosis of chronic lymphocytic leukaemia cells by autologous macrophages. *Clin Exp Immunol, 183*(1), 90-101. doi:10.1111/cei.12697

Dahal, L. N., Dou, L., Hussain, K., Liu, R., Earley, A., Cox, K. L., . . . Beers, S. A. (2017). STING Activation Reverses Lymphoma-Mediated Resistance to Antibody Immunotherapy. *Cancer Res, 77*(13), 3619-3631. doi:10.1158/0008-5472.CAN-16-2784

Dahal, L. N., Huang, C. Y., Stopforth, R. J., Mead, A., Chan, K., Bowater, J. X., . . . Beers, S. A. (2018). Shaving Is an Epiphenomenon of Type I and II Anti-CD20-Mediated Phagocytosis, whereas Antigenic Modulation Limits Type I Monoclonal Antibody Efficacy. *J Immunol, 201*(4), 1211-1221. doi:10.4049/jimmunol.1701122

Dominguez, R., & Holmes, K. C. (2011). Actin structure and function. *Annu Rev Biophys, 40*, 169-186. doi:10.1146/annurev-biophys-042910-155359

Eden, S., Rohatgi, R., Podtelejnikov, A. V., Mann, M., & Kirschner, M. W. (2002). Mechanism of regulation of WAVE1-induced actin nucleation by Rac1 and Nck. *Nature, 418*(6899), 790-793. doi:10.1038/nature00859

Egile, C., Rouiller, I., Xu, X. P., Volkmann, N., Li, R., & Hanein, D. (2005). Mechanism of filament nucleation and branch stability revealed by the structure of the Arp2/3 complex at actin branch junctions. *PLoS Biol, 3*(11), e383. doi:10.1371/journal.pbio.0030383

Elizabeth, M. B., Amit, C., Harika, V., Daniel, O., John, S., Anthony, M. M., . . . Adam, D. H. (2020). Engineered IgG1-Fc molecules define valency control of cell surface Fcg receptor inhibition and activation in endosomes. *Front Immunol*.

Fletcher, D. A., & Mullins, R. D. (2010). Cell mechanics and the cytoskeleton. *Nature, 463*(7280), 485-492. doi:10.1038/nature08908

Frank, M., Egile, C., Dyachok, J., Djakovic, S., Nolasco, M., Li, R., & Smith, L. G. (2004). Activation of Arp2/3 complex-dependent actin polymerization by plant proteins distantly related to Scar/WAVE. *Proc Natl Acad Sci U S A, 101*(46), 16379-16384. doi:10.1073/pnas.0407392101

Goley, E. D., Rammohan, A., Znameroski, E. A., Firat-Karalar, E. N., Sept, D., & Welch, M. D. (2010). An actin-filament-binding interface on the Arp2/3 complex is critical for nucleation and branch stability. *Proc Natl Acad Sci U S A, 107*(18), 8159-8164. doi:10.1073/pnas.0911668107

Goodridge, H. S., Reyes, C. N., Becker, C. A., Katsumoto, T. R., Ma, J., Wolf, A. J., . . . Underhill, D. M. (2011). Activation of the innate immune receptor Dectin-1 upon formation of a 'phagocytic synapse'. *Nature, 472*(7344), 471-475. doi:10.1038/nature10071

Gordan, S., Biburger, M., & Nimmerjahn, F. (2015). bIgG time for large eaters: monocytes and macrophages as effector and target cells of antibody-mediated

immune activation and repression. *Immunol Rev, 268*(1), 52-65. doi:10.1111/imr.12347

Gordon, S. R., Maute, R. L., Dulken, B. W., Hutter, G., George, B. M., McCracken, M. N., . . . Weissman, I. L. (2017). PD-1 expression by tumour-associated macrophages inhibits phagocytosis and tumour immunity. *Nature, 545*(7655), 495-499. doi:10.1038/nature22396

Grakoui, A., Bromley, S. K., Sumen, C., Davis, M. M., Shaw, A. S., Allen, P. M., & Dustin, M. L. (1999). The immunological synapse: a molecular machine controlling T cell activation. *Science, 285*(5425), 221-227. doi:10.1126/science.285.5425.221

Griffin, F. M., Jr., Griffin, J. A., Leider, J. E., & Silverstein, S. C. (1975). Studies on the mechanism of phagocytosis. I. Requirements for circumferential attachment of particle-bound ligands to specific receptors on the macrophage plasma membrane. *J Exp Med, 142*(5), 1263-1282. doi:10.1084/jem.142.5.1263

Griffin, F. M., Jr., Griffin, J. A., & Silverstein, S. C. (1976). Studies on the mechanism of phagocytosis. II. The interaction of macrophages with anti-immunoglobulin IgG-coated bone marrow-derived lymphocytes. *J Exp Med, 144*(3), 788-809. doi:10.1084/jem.144.3.788

Guillen, N. (2014). Infection biology: Nibbled to death. *Nature, 508*(7497), 462-463. doi:10.1038/nature13223

Gul, N., & van Egmond, M. (2015). Antibody-Dependent Phagocytosis of Tumor Cells by Macrophages: A Potent Effector Mechanism of Monoclonal Antibody Therapy of Cancer. *Cancer Res, 75*(23), 5008-5013. doi:10.1158/0008-5472.CAN-15-1330

He, W., Chen, C. J., Mullarkey, C. E., Hamilton, J. R., Wong, C. K., Leon, P. E., . . . Tan, G. S. (2017). Alveolar macrophages are critical for broadly-reactive antibody-mediated protection against influenza A virus in mice. *Nat Commun, 8*(1), 846. doi:10.1038/s41467-017-00928-3

Holowka, D., Sil, D., Torigoe, C., & Baird, B. (2007). Insights into immunoglobulin E receptor signaling from structurally defined ligands. *Immunol Rev, 217*, 269-279. doi:10.1111/j.1600-065X.2007.00517.x

Jaumouille, V., Farkash, Y., Jaqaman, K., Das, R., Lowell, C. A., & Grinstein, S. (2014). Actin cytoskeleton reorganization by Syk regulates Fcgamma receptor responsiveness by increasing its lateral mobility and clustering. *Dev Cell, 29*(5), 534-546. doi:10.1016/j.devcel.2014.04.031

Kim, A. S., Kakalis, L. T., Abdul-Manan, N., Liu, G. A., & Rosen, M. K. (2000). Autoinhibition and activation mechanisms of the Wiskott-Aldrich syndrome protein. *Nature, 404*(6774), 151-158. doi:10.1038/35004513

Kotila, T., Wioland, H., Enkavi, G., Kogan, K., Vattulainen, I., Jegou, A., . . . Lappalainen, P. (2019). Mechanism of synergistic actin filament pointed end depolymerization by cyclase-associated protein and cofilin. *Nat Commun, 10*(1), 5320. doi:10.1038/s41467-019-13213-2

Li, X., & Kimberly, R. P. (2014). Targeting the Fc receptor in autoimmune disease. *Expert Opin Ther Targets, 18*(3), 335-350. doi:10.1517/14728222.2014.877891

Lin, J., & Hoppe, A. D. (2013) Uniform total internal reflection fluorescence illumination enables live cell fluorescence resonance energy transfer microscopy. (1435-8115 (Electronic)).

Lin, J., Kurilova, S., Scott, B. L., Bosworth, E., Iverson, B. E., Bailey, E. M., & Hoppe, A. D. (2016). TIRF imaging of Fc gamma receptor microclusters dynamics and signaling on macrophages during frustrated phagocytosis. *BMC Immunol, 17*, 5. doi:10.1186/s12865-016-0143-2

Lin, K. B., Freeman, S. A., Zabetian, S., Brugger, H., Weber, M., Lei, V., . . . Gold, M. R. (2008). The rap GTPases regulate B cell morphology, immune-synapse formation, and signaling by particulate B cell receptor ligands. *Immunity, 28*(1), 75-87. doi:10.1016/j.immuni.2007.11.019

Linder, S., & Wiesner, C. (2015). Tools of the trade: podosomes as multipurpose organelles of monocytic cells. *Cell Mol Life Sci, 72*(1), 121-135. doi:10.1007/s00018-014-1731-z

Liu, C., Bai, X., Wu, J., Sharma, S., Upadhyaya, A., Dahlberg, C. I., . . . Song, W. (2013). N-wasp is essential for the negative regulation of B cell receptor signaling. *PLoS Biol, 11*(11), e1001704. doi:10.1371/journal.pbio.1001704

Lou, J., Low-Nam, S. T., Kerkvliet, J. G., & Hoppe, A. D. (2014). Delivery of CSF-1R to the lumen of macropinosomes promotes its destruction in macrophages. *J Cell Sci, 127*(Pt 24), 5228-5239. doi:10.1242/jcs.154393

Lowell, C. A. (2011). Src-family and Syk kinases in activating and inhibitory pathways in innate immune cells: signaling cross talk. *Cold Spring Harb Perspect Biol, 3*(3). doi:10.1101/cshperspect.a002352

Machesky, L. M., Mullins, R. D., Higgs, H. N., Kaiser, D. A., Blanchoin, L., May, R. C., . . . Pollard, T. D. (1999). Scar, a WASp-related protein, activates nucleation of actin filaments by the Arp2/3 complex. *Proc Natl Acad Sci U S A, 96*(7), 3739-3744. doi:10.1073/pnas.96.7.3739

Marshall, M. J. E., Stopforth, R. J., & Cragg, M. S. (2017). Therapeutic Antibodies: What Have We Learnt from Targeting CD20 and Where Are We Going? *Front Immunol, 8*, 1245. doi:10.3389/fimmu.2017.01245

Matlung, H. L., Babes, L., Zhao, X. W., van Houdt, M., Treffers, L. W., van Rees, D. J., . . . van den Berg, T. K. (2018). Neutrophils Kill Antibody-Opsonized Cancer Cells by Trogoptosis. *Cell Rep, 23*(13), 3946-3959 e3946. doi:10.1016/j.celrep.2018.05.082

McQuin, C., Goodman, A., Chernyshev, V., Kamentsky, L., Cimini, B. A., Karhohs, K. W., . . . Carpenter, A. E. (2018). CellProfiler 3.0: Next-generation image processing for biology. *PLoS Biol, 16*(7), e2005970. doi:10.1371/journal.pbio.2005970

Millard, T. H., Sharp, S. J., & Machesky, L. M. (2004). Signalling to actin assembly via the WASP (Wiskott-Aldrich syndrome protein)-family proteins and the Arp2/3 complex. *Biochem J, 380*(Pt 1), 1-17. doi:10.1042/BJ20040176

Mocsai, A., Ruland, J., & Tybulewicz, V. L. (2010). The SYK tyrosine kinase: a crucial player in diverse biological functions. *Nat Rev Immunol, 10*(6), 387-402. doi:10.1038/nri2765

Morrissey, M. A., Williamson, A. P., Steinbach, A. M., Roberts, E. W., Kern, N., Headley, M. B., & Vale, R. D. (2018). Chimeric antigen receptors that trigger phagocytosis. *Elife, 7*. doi:10.7554/eLife.36688

Mullarkey, C. E., Bailey, M. J., Golubeva, D. A., Tan, G. S., Nachbagauer, R., He, W., . . . Palese, P. (2016). Broadly Neutralizing Hemagglutinin Stalk-Specific

Antibodies Induce Potent Phagocytosis of Immune Complexes by Neutrophils in an Fc-Dependent Manner. *mBio, 7*(5). doi:10.1128/mBio.01624-16

Mullins, R. D., Heuser, J. A., & Pollard, T. D. (1998). The interaction of Arp2/3 complex with actin: nucleation, high affinity pointed end capping, and formation of branching networks of filaments. *Proc Natl Acad Sci U S A, 95*(11), 6181-6186. doi:10.1073/pnas.95.11.6181

Pantaloni, D., Boujemaa, R., Didry, D., Gounon, P., & Carlier, M. F. (2000). The Arp2/3 complex branches filament barbed ends: functional antagonism with capping proteins. *Nat Cell Biol, 2*(7), 385-391. doi:10.1038/35017011

Pham, T., Mero, P., & Booth, J. W. (2011). Dynamics of macrophage trogocytosis of rituximab-coated B cells. *PLoS One, 6*(1), e14498. doi:10.1371/journal.pone.0014498

Planchon, T. A., Gao, L., Milkie, D. E., Davidson, M. W., Galbraith, J. A., Galbraith, C. G., & Betzig, E. (2011). Rapid three-dimensional isotropic imaging of living cells using Bessel beam plane illumination. *Nat Methods, 8*(5), 417-423. doi:10.1038/nmeth.1586

Pollard, T. D., & Borisy, G. G. (2003). Cellular motility driven by assembly and disassembly of actin filaments. *Cell, 112*(4), 453-465. doi:10.1016/s0092-8674(03)00120-x

Pollitt, A. Y., & Insall, R. H. (2009). WASP and SCAR/WAVE proteins: the drivers of actin assembly. *J Cell Sci, 122*(Pt 15), 2575-2578. doi:10.1242/jcs.023879

Rey-Suarez, I., Wheatley, B. A., Koo, P., Bhanja, A., Shu, Z., Mochrie, S., . . . Upadhyaya, A. (2020). WASP family proteins regulate the mobility of the B cell receptor during signaling activation. *Nat Commun, 11*(1), 439. doi:10.1038/s41467-020-14335-8

Rotty, J. D., Wu, C., & Bear, J. E. (2013). New insights into the regulation and cellular functions of the ARP2/3 complex. *Nat Rev Mol Cell Biol, 14*(1), 7-12. doi:10.1038/nrm3492

Sancak, Y., Peterson, T. R., Shaul, Y. D., Lindquist, R. A., Thoreen, C. C., Bar-Peled, L., & Sabatini, D. M. (2008). The Rag GTPases bind raptor and mediate amino acid signaling to mTORC1. *Science, 320*(5882), 1496-1501. doi:10.1126/science.1157535

Schindelin, J., Arganda-Carreras, I., Frise, E., Kaynig, V., Longair, M., Pietzsch, T., . . . Cardona, A. (2012). Fiji: an open-source platform for biological-image analysis. *Nat Methods, 9*(7), 676-682. doi:10.1038/nmeth.2019

Shapouri-Moghaddam, A., Mohammadian, S., Vazini, H., Taghadosi, M., Esmaeili, S. A., Mardani, F., . . . Sahebkar, A. (2018). Macrophage plasticity, polarization, and function in health and disease. *J Cell Physiol, 233*(9), 6425-6440. doi:10.1002/jcp.26429

Sips, M., Krykbaeva, M., Diefenbach, T. J., Ghebremichael, M., Bowman, B. A., Dugast, A. S., . . . Alter, G. (2016). Fc receptor-mediated phagocytosis in tissues as a potent mechanism for preventive and therapeutic HIV vaccine strategies. *Mucosal Immunol, 9*(6), 1584-1595. doi:10.1038/mi.2016.12

Stanford, S. M., Rapini, N., & Bottini, N. (2012). Regulation of TCR signalling by tyrosine phosphatases: from immune homeostasis to autoimmunity. *Immunology, 137*(1), 1-19. doi:10.1111/j.1365-2567.2012.03591.x

Stewart, S. A., Dykxhoorn, D. M., Palliser, D., Mizuno, H., Yu, E. Y., An, D. S., . . . Novina, C. D. (2003). Lentivirus-delivered stable gene silencing by RNAi in primary cells. *RNA, 9*(4), 493-501. doi:10.1261/rna.2192803

Swanson, J. A., & Hoppe, A. D. (2004). The coordination of signaling during Fc receptor-mediated phagocytosis. *J Leukoc Biol, 76*(6), 1093-1103. doi:10.1189/jlb.0804439

Takenawa, T., & Suetsugu, S. (2007). The WASP-WAVE protein network: connecting the membrane to the cytoskeleton. *Nat Rev Mol Cell Biol, 8*(1), 37-48. doi:10.1038/nrm2069

Tsai, R. K., & Discher, D. E. (2008). Inhibition of "self" engulfment through deactivation of myosin-II at the phagocytic synapse between human cells. *J Cell Biol, 180*(5), 989-1003. doi:10.1083/jcb.200708043

Vaughan, A. T., Chan, C. H., Klein, C., Glennie, M. J., Beers, S. A., & Cragg, M. S. (2015). Activatory and inhibitory Fcgamma receptors augment rituximab-mediated internalization of CD20 independent of signaling via the cytoplasmic domain. *J Biol Chem, 290*(9), 5424-5437. doi:10.1074/jbc.M114.593806

Velmurugan, R., Challa, D. K., Ram, S., Ober, R. J., & Ward, E. S. (2016). Macrophage-Mediated Trogocytosis Leads to Death of Antibody-Opsonized Tumor Cells. *Mol Cancer Ther, 15*(8), 1879-1889. doi:10.1158/1535-7163.MCT-15-0335

Watrach, A. M., Hanson, L. E., & Watrach, M. A. (1963). The Structure of Infectious Laryngotracheitis Virus. *Virology, 21*, 601-608. doi:10.1016/0042-6822(63)90233-2

Weiskopf, K., & Weissman, I. L. (2015). Macrophages are critical effectors of antibody therapies for cancer. *MAbs, 7*(2), 303-310. doi:10.1080/19420862.2015.1011450

Woof, J. M., & Burton, D. R. (2004). Human antibody-Fc receptor interactions illuminated by crystal structures. *Nat Rev Immunol, 4*(2), 89-99. doi:10.1038/nri1266

CHAPTER II. IGG MOBILITY ON THE TARGET SURFACE AFFECT FCγ RECEPTOR MEDIATED PHAGOCYTIC SIGNAL

Abstract

Antibody dependent cellular phagocytosis (ADCP) is an important effector mechanism for the removal of malignant and infected host cells during treatment with therapeutic antibodies or adaptive immune responses. Many antigens on the surface of host cells are mobile with diffusion limited by transient interactions with the cytoskeleton. However, ADCP has largely been studied using target particles that display immobile antigens. Here, we found that during ADCP, antigen-IgG is dramatically rearranged by the phagocyte and that increasing surface mobility predicts ADCP efficiency. Using confocal and lattice light sheet microscopy, we show that during ADCP of B-lymphoma cells (WIL2-S), macrophages rearrange Fc receptor (FcγR)-IgG-CD20 microclusters, initially accumulating them in patches at the base of the phagocytic cup and subsequently dispersing them coincident with the formation of new ones at the advancing edge of the forming phagosome. This process was distinct from the engagement of immobile IgG and involved and dynamic regulation of topography in contact with the target. Specifically, depolymerization of the actin cytoskeleton in WIL2-S cells resulted in free diffusion of IgG-CD20, which in turn enhanced microcluster reorganization, Syk recruitment, and ADCP efficiency. Conversely, immobilization of IgG-CD20 impaired FcγR-IgG microcluster reorganization and Syk recruitment resulting in diminished ADCP. In macrophages lacking Syk, FcγR-IgG patches were accumulated at the base of the phagosome and failed to rearrange. These patches were efficiently trogocytosed, leading

to release of the WIL2-S cells. Additionally, inhibition of Arp2/3 in macrophages impaired reorganization of FcγR-IgG microclusters, Syk recruitment, and pseudopod extension around the target. Thus, we conclude that Syk and Arp2/3 coordination of FcγR-IgG microcluster reorganization and signal amplification is a critical activity for ADCP and that this pathway is ideally adapted for recognition of surface-mobile IgG.

INTRODUCTION

Therapeutic antibodies are a rapidly growing class of drugs for treating rheumatological, viral, and malignant diseases (Ackerman et al., 2013; Marshall, Stopforth, & Cragg, 2017; Sips et al., 2016). Nearly all are of class IgG owing to long circulatory half-lives, broad tissue distribution, and the ability to activate potent immune effector functions on cells bearing Fcγ receptors (FcγR) (Gordan et al., 2015; He et al., 2017; Marshall et al., 2017; Mullarkey et al., 2016). A growing body of evidence indicates that Antibody Dependent Cellular Phagocytosis (ADCP) by macrophages and monocytes is an important or essential effector mechanism, especially for the destruction of targets of lymphocytic origin (C. Alvey & Discher, 2017; Brandsma et al., 2018; Dahal et al., 2017; Gordan et al., 2015; Gul & van Egmond, 2015; He et al., 2017; Weiskopf & Weissman, 2015). Some of the most successful therapeutic antibodies that mediate ADCP killing of lymphocytes includes anti-CD20 (Rituximab) and its derivatives, and anti-CD52 (Alemtuzumab) (Church et al., 2016; Dahal et al., 2018; Vaughan et al., 2015). Ineffective ADCP leads to trogocytosis in which effector cells take small bites of the target cell's plasma membrane leading to antigenic modulation and promoting escape of the therapeutic target (Barkal et al., 2018; Chao et al., 2010; Gordon et al., 2017; Shapouri-Moghaddam et al., 2018) or, conversely, may facilitate killing large target cells including breast cancer cells (Matlung et al., 2018; Velmurugan, Challa, Ram, Ober, & Ward, 2016). Thus, there is a pressing need to understand the cellular and molecular mechanisms by which FcγR ligation to target-bound IgG orchestrates effective ADCP and how the antigen on the target cell influences this process to enable the development of improved therapeutic antibodies and adjuvants.

Macrophages, monocytes, and dendritic cells express all FcγRs to varying degrees and are resident in nearly all tissues of the body making them key effectors of IgG-mediated responses and antigen presentation (Barkal et al., 2018; Dahal et al., 2017; Gordan et al., 2015; Gordon et al., 2017; Shapouri-Moghaddam et al., 2018; Weiskopf & Weissman, 2015). A growing body of literature indicates that macrophage ADCP can also be an effective mechanism for antibody mediated anti-tumor activity provided that inhibitory signals originating from the microenvironment are overcome (C. Alvey & Discher, 2017; C. M. Alvey et al., 2017; Chao et al., 2010; Gordon et al., 2017; Tsai & Discher, 2008; Weiskopf & Weissman, 2015), including the use of STING agonists and CD47/SIRPα blocking antibodies to potentiate ADCP in tumor microenvironments (Barkal et al., 2018; Boudreau & Alter, 2019; Church et al., 2016; Gordon et al., 2017). Recently, the concept of engineering macrophages with chimeric antigen receptors, analogous to CAR-T cells, as an alternative cell-based therapeutic strategy has emerged (Morrissey et al., 2018), further highlighting the need to understand the molecular mechanisms regulating macrophage ADCP. Our understanding of ADCP and the mechanisms underpinning its efficacy and failure are shaped by the two historical models of phagocytosis known as the 'zipper' and the 'trigger'(Griffin, Griffin, Leider, & Silverstein, 1975; Griffin, Griffin, & Silverstein, 1976; Swanson & Hoppe, 2004). The zipper model posits that FcγRs must sequentially engage IgG on the target surface as actin polymerization extends membrane over the target, similar to the closing of a zipper (Griffin et al., 1976). In contrast, the trigger model posits that if sufficient FcγRs bind IgG that an activating signal will trigger large-scale cytoskeletal rearrangements to engulf the target. In seminal work from the Silverstein lab, the zipper model prevailed, as targets that 'capped' or sequestered anti-Ig (presumably

anti-surface Ig) into a sub-region of the lymphocyte surface could not mediate ADCP by macrophages but the IgG was efficiently internalized by trogocytosis. Importantly, successful ADCP required new FcγR engaging with IgG on the target outside of the initial phagocytic synapse (Griffin et al., 1976). Thus, it appeared that targets that rearrange antigen-IgG complexes on their surface can influence ADCP and trogocytosis (Pham, Mero, & Booth, 2011), with diffuse IgG distributions associated with ADCP (Griffin et al., 1976). However, antigens such as CD20, CD52, and EGFR are mobile, and microclustering and segregation of IgG-FcγR driven by the phagocyte has been observed for these cellular targets on synthetic membranes (Bakalar et al., 2018; Linder & Wiesner, 2015). Understanding mechanisms of FcγR-mediated phagocytosis will provide critical information for the rational design of next-generation therapeutic antibodies including establishing criteria for antigen selection, optimal antibody Fc structure, and complementary adjuvant therapies to promote ADCP.

Here, we have addressed the cellular rearrangements of IgG and FcγRs at the macrophage/target cell interface during ADCP. Our findings indicate that for CD20, the surface mobility of the IgG/FcγR complex has a profound effect on successful ADCP, with increased surface mobility corresponding to higher likelihood of successful ADCP. Moreover, we find that Syk and Arp2/3 are required to maintain IgG-FcγR complexes near the advancing edge of the pseudopod and to limit trogocytic clearance of IgG from the target.

Methods

Cell Culture

Fetal liver-derived macrophages (FLMs) were prepared from E18 mouse fetuses from B6J.129(Cg)-Igs2tm1.1(CAG-cas9*)Mmw/J mice (The Jackson Laboratory, Stock No. 028239, Bar Harbor, ME) with South Dakota State University Institutional Animal Use and Care Committee approval. Liver tissue was mechanically dissociated using sterile fine-pointed forcepts and a single cell suspensions was created by passing the tissue through a 1mL pipette tip. Bone marrow-derived macrophages (BMDMs) were prepared using single cell suspensions of bone marrow obtained from the long bones of B6J.129(Cg)-Gt(ROSA)26Sortm1.1(CAG-cas9*,-EGFP)Fezh/J (The Jackson Laboratory, Stock No. 026179, Bar Harbor, ME). BMDM and FLMs were cultured in bone marrow media containing DMEM (Corning) supplemented with 30% L cell supernatant, 20% Heat-inactivated FBS (R&D Systems) and 1% pen/strep (ThermoFisher) and incubated at 37C and 5% CO_2. WIL2-S cells were cultured in RPMI-1640 medium (ATCC 30-2001) containing 10% FBS and 1% pen/strep (ThermoFisher) at 37˚C with 5% CO_2. WIL2-S cells were used for phagocytosis assays and live imaging.

Plasmids, lentiviral transduction and CRISPR gene disruption

Lentiviral expression plasmids, pLJM1-AktPH-mScarlet, pLJM1-Syk-mScarlet, and pLJM1-Lyk(mem)-mNeonGreen were created by gene synthesis (GeneScript). Lentiviral vectors were produced in 293T cells by transfection with pLJM-Syk-mScarlet-1 and pLJM-AktPH-mScarlet in combination with helper plasmids pPAX2 (Addgene plasmid # 12260) and pVSVG (Addgene plasmid 242 #8454), using polyethylenimine (PEI). After 48 h, lentivirus was harvested, centrifuged, and added to FLM cells. After the 48-hour transduction, cells were selected with Blasticidin (10 μg/mL) and/or Puromycin (5 μg/mL)

for two days. Macrophages were split into respective well formats for experiments. Once BMMs or FLMs reached appropriate seeding density, they were used for phagocytosis assays, frustrated phagocytosis and live imaging.

Antibody labeling with NHS ester fluorophores

Both Rituximab (anti-CD20 – murine IgG2a, hcd20-mab10, InvivoGen) and monoclonal mouse anti-Biotin IgG2a [3E6] (ab36406, Abcam) were fluorescently labeled using Alexa Fluor 647 NHS ester (Thermo Fisher scientific), or CF647 NHS ester (Biotium). Prior to labeling, antibodies were buffer exchanged in Zeba Spin desalting columns (ThermoFisher) with three washes of PBS, pH 7.4 without Ca^{2+} and Mg^{2+} (ThermoFisher). Exchanged antibodies were mixed with NHS-fluorophore at molar ratio of 1:10 IgG:fluorophore in 0.1M sodium bicarbonate solution (ThemoFisher) with pH of 8.1-8.3. The mixture was incubated for 1 hour at room temperature. After 1 hour incubation, excess fluorophores in the solution were removed using Zeba Spin columns.

Supported Lipid Bilayers

Bilayers were formed by spontaneous fusion of lipid vesicles. Small unilamellar vesicles (SUVs) were prepared by mixing DSPE-PEG(2000) Biotin (880129 Avanti Polar Lipids) and DPPC (850355 Avanti Polar Lipids) or POPC (850457 Avanti Polar Lipids) at a molar ratio of 1:1000 with total lipid concentration of 500 μM (380 μg/mL) in chloroform. Lipids were then roto-vacuum dried for up to 60 min in a glass test tube. The lipid film was resuspended using 1 mL PBS, pH 7.4 without Ca^{2+} and Mg^{2+}. The glass tube was then sonicated for 5 minutes using a bath sonicator (JSP US40) followed by extrusion (610000 Avanti Polar Lipids) through 100 nm filter at least 13 times (Whatman Nucleopore Track-Etch 100 nm membrane). POPC liposomes, T_m of -2˚C, were extruded and sonicated at

room temperature, whereas DPPC liposomes with T_m of 41˚C, were extruded and sonicated at 60˚C.

The 500 μM stock of SUVs were diluted 1:6 in 2mM Mg^{2+} PBS. POPC SLBs were formed by pipetting the diluted lipids onto Hellmanex III (MilliporeSigma) cleaned 96-well plates and incubated at 37ºC for 30 minutes. DPPC bilayers were formed by pipetting the diluted lipids onto 25 mm Hellmanex III (MilliporeSigma) cleaned coverslip mounted in a pre-warmed Attofluor chamber (ThermoFisher) and incubated at 70ºC for 30 minutes on a slide-warmer (Premier XH-2001). Bilayers were also formed on silica beads with 5 μm diameter (Bangs Laboratories). Silica beads were washed by centrifugation twice with 100% acetone, twice with 100% ethanol and twice with 100% deionized water. POPC and DPPC SUVs were then incubated at 37ºC or 70ºC for 30 minutes with the cleaned silica beads. Following incubation, excess liposomes were removed by pipetting in Hank's Balanced Salt Solution (HBSS, Corning™ 21023CV) containing FBS in 1:1000 ratio (HBSS+0.1% FBS). SLBs and SLB-SBs were incubated with anti-Biotin IgG (3E6) (Abcam ab36406) conjugated with Alexa Fluor 647 NHS ester (Thermo Fisher scientific) SLB at 37 °C for 30 min. SLBs were rinsed without exposure to air to remove excess IgG using HBSS.

For imaging FLM cells on SLBs, SLBs were made directly on Hallmanex III (MilliporeSigma) cleaned 25 mm coverslips (Number 1.5, Thermo Fisher) or onto 96-well glass bottom plates (Dot Scientific, MGB096-1-2-LG-L) for high content experiments. The 25 mm coverslips were imaged in AttoFluor chambers (Thermo Fisher). To measure spreading area, images were taken 10 minutes after dropping macrophages on SLBs for 5-8 minutes. The spreading area was manually measured by thresholding on ImageJ Fiji (Schindelin et al., 2012).

Drug Treatment on cells

Paraformaldehyde (PFA, T353-500, ThermoFisher), Latrunculin B (Lat B, 428020, MilliporeSigma) and Jasplakinolide (Jas, 420107, MilliporeSigma)/Blebbistatin (Bleb, B0560, Sigma-Aldrich) were used to alter CD20 mobility on the surface of WIL2-S. 4% PFA was prepared using powder form PFA which was diluted to prepare 2% PFA using PBS, pH 7.4 without Ca^{2+} and $Mg^{2+}$and stored at -20°C. WIL2-S cells were treated using 2% PFA for 10 minutes in 4°C. Lat B was resuspended in DMSO at a concentration of 62.5 mM (25 mg/mL) and stored at -20°C. 12.5 mM Lat B solution was prepared from the stock solution and used to treat WIL2-S cells for 30 minutes at 4°C. Jas and Bleb were stored in DMSO with concentration of 1mM (0.71 mg/mL) and 17mM (5 mg/mL) at -20 °C. Cells were then incubated with 75 μM Bleb for 10 minutes, followed by 1μM Jas for 5 minutes. After drug treatment, WIL2-S cells were thoroughly washed by centrifugation 3 times and incubated on ice.

FLMs were treated with CK 666 (MilliporeSigma) for live imaging. Commercially purchased CK 666 was stored in DMSO with the concentration of 85mM (25 mg/mL), at 4 °C. FLMs were treated with 1.2 μM CK 666 in HBSS for 1 hour at 4 °C before live imaging.

Live Imaging

FLMs were dropped onto prepared SLBs. TIRF-based imaging was conducted using an inverted microscope built around a Till iMic (Till Photonics, Germany) equipped with a 60x 1.49 N.A. oil immersion objective lens. The entire microscope setup and centering of the back focal plane was previously described previously (Scott et al., 2018). Cells were labeled using 1μg/mL DiI in 2.5% DMSO/PBS. Excitation for TIRF was provided by a

633nm laser for AF 647 anti-biotin mIgG2a, or a 561 nm laser for DiI or Syk-mScarlet or Akt-mScarlet, or a 488 nm laser for Mem-mNG.

TIRF 360 was used to create uniform TIRF illumination for fluorescence recovery after photobleaching (FRAP) by steering the laser at the back-focal plane (J. Lin et al., 2016). The microscope was custom-built based on iMIC system (TILL Photonics, Munich, Germany) with 60x 1.49 oil immersion objective lens (Olympus, Tokyo, Japan). Spreading area and mobile fraction were measured using ImageJ Fiji (Schindelin et al., 2012). For spreading area, thresholding was used to make ROIs around cells. Mobile fraction was calculated by measuring and comparing change in intensity overtime on photobleached spots and backgrounds.

For confocal imaging, FLMs plated on ethanol flamed 25 mm coverslips were challenged by WIL2-S cells. Imaging was performed on a TIL photonics Andromeda Spinning Disk Confocal (TILL Photonics, Munich, Germany), using a 60x oil 1.4 oil immersion objective lens. Excitation for confocal imaging was provided by a 640 nm laser for AF 647 anti-CD20 mIgG2a, or a 561 nm laser for Syk-mScarlet, or Mem-mScarlet, or a 515 nm laser for Mem-mNG. Cells were incubated in HBSS during imaging.

High Content Imaging

For high content experiments, BMDM were plated on 96-well plates for at least 2 hours (Dot Scientific, MGB096-1-2-LG-L). Before imaging, WIL2-S cells were treated with WIL2-S cells opsonized with various concentrations of anti-human CD20 – murine IgG2a (hcd20-mab10, InvivoGen) and washed 2 times. WIL2-S cells were then treated with different drugs including PFA, Lat B and Jas/Bleb which were washed three times. WIL2-S cells were labeled using pHrodo™ SE Red dye (ThermoFisher) in PBS, pH 7.4 without

Ca^{2+} and Mg^{2+} and washed 3 times. Media was exchanged using HBSS for imaging by centrifugation. High content fluorescent imaging was conducted using an ImageXpress Micro XLS Widefield High-Content Analysis System (Molecular Devices, Sunnyvale, CA) equipped with a 20 × 0.70 N.A. objective lens. For each well, 6 field of views were used. Excitation was (Ex 562/40, Em 624/40) for pHrodoRed, (Ex 482/35, Em 536/40) for Cas9 GFP, or (Ex 377/50, Em 447/60) for HCS NuclearMask™ Blue Stain (ThermoFisher). Images were analyzed using CellProfiler Analyst software to obtain the number of engulfed WIL2-S cells per macrophage which is called phagocytic index (PI) by using a pre-built pipeline (McQuin et al., 2018). Graphs were made in MATLAB (The MathWorks Inc, Natick, MA).

The density of IgG on cells were measured using Alexa Fluor 633 Goat anti-Mouse IgG2a Cross-Adsorbed Secondary Antibody (ThermoFisher). Secondary antibody was diluted in HBSS+0.1% FBS, 1:1000. Opsonized WIL2-S cells for high content imaging were incubated in the diluted secondary antibody for 30 minutes, washed 3 times with HBSS, cells were run on BD Accuri™ C6 Plus Flow Cytometer. All data from flow cytometer was edited using BD FlowJo™ software and MATLAB (The MathWorks Inc, Natick, MA).

Lattice Light Sheet Microscopy Imaging.

The LLSM is a replica of the design described by Chen et al.(B. C. Chen et al., 2014), built under license from HHMI. Volumetric image stacks were generated using dithered square virtual lattices (Outer NA 0.55, Inner NA 0.50, approximately 30 μm long) and stage scanning with 0.5 μm step sizes, resulting in 254 nm deskewed z-steps. The typical field of view was 768x768 pixels and 151 slices which corresponding to ~76μm x 76μm x 42μm with an imaging rate of 10-12 seconds per volume. Excitation laser powers used were

0.58μW (405 nm), 15 μW (488 nm), 22 μW (560 nm) and 17μW (640 nm) as measured at the back aperture of the excitation objective. The optimized laser powers resulted sufficient SNR for imaging and less than 10% bleaching throughout the 150 frame movies. The emission filter cube (DFM1, Thorlabs) comprised a quadband notch filter NF03-405/488/561/635 (Semrock), longpass dichroic mirror Di02-R561 (Semrock), shortpass filter 550SP (Omega) on the reflected path, and longpass filter BLP01-561R (Semrock) on the transmitted path; the resulting fluorescence was imaged onto a pair of ORCA-Flash4.0 v2 sCMOS cameras (Hamamatsu). The camera on the reflected image path was mounted on a manual x-y-z translation stage (Newport 462-XYZ stage, Thorlabs), and the images were registered using 0.1 μm Fluoresbrite YG microspheres (Polysciences). Representative fields of view were chosen before $3x10^5$ WIL2-S cells were dropped on top of the FLMs and imaging began within a minute of addition.

Deconvolution and Post Processing.

The processing and viewing in ChimeraX was described previously(Quinn et al., 2020). Briefly, the raw volumes acquired from the LLSM were deskewed, deconvolved, and rotated to coverslip coordinates in LLSpy(Lambert & Shao, 2019). We applied a fixed background subtraction based on an average dark current image, 10 iterations of Lucy-Richardson deconvolution with experimentally measured point spread functions for each excitation, followed by rotation to coverslip coordinates and cropping to the region of interest. The fully preprocessed data was loaded into ChimeraX for visualization through a combination of volumetric intensity projections, isosurface, or mesh renderings.

RESULTS

Macrophages rearrange Rituximab-CD20 into microclusters during ADCP of B lymphoma cells.

We first sought to determine how IgG was organized at the phagocytic synapse during ADCP. Given our prior findings that IgG presented on supported lipid bilayers was rearranged following engagement of macrophage FcγR in a process reminiscent of TCR and BCR rearrangements, we hypothesized that similar rearrangements occur during ADCP (J. Lin et al., 2016). We focused on Rituximab, which is thought to mediate ADCP of CD20 positive cells (Boross et al., 2011; Church et al., 2016; Minard-Colin et al., 2008). Indeed, confocal microscopy of Rituximab (murine IgG2a) labeled with AlexaFluor (Rtx-647) revealed the formation of microclusters at the target-contact interface, with the highest fluorescence intensity at the base of phagocytic synapse where they recruited a previously validated Syk-mScarlet chimera (Bailey et al., 2020) (Fig. 1). During engulfment, these microclusters redistributed over the surface of the WIL2-S target as the enveloping pseudopod advanced, ultimately resulting in a phagosome containing the WIL2-S target with an approximately uniform distribution of Rtx-647 microclusters that co-localized with Syk-mScarlet (Fig. 1A). To gain a more complete three-dimensional view of this process, we applied lattice light sheet microscopy (LLSM), which is capable of capturing 3D imaging volumes with minimal photoxicity at high imaging frame rates (B. C. Chen et al., 2014; Planchon et al., 2011). LLSM imaging revealed that the Rtx-647 was present on the surface of isolated WIL2-S as a mixture of punctate and uniform distributions, but upon contact with the macrophage formed microclusters that rapidly recruited Syk-mScarlet (Fig. 1B). As the phagosome cup began

to form, microclusters were observed to stream toward the base of the phagosome (i.e., the initial contact site) suggesting a potential coupling between the macrophage FcγRs and the retrograde flow of the actin cytoskeleton. Within 1-2 min post contact, small membrane ruffles, not attached to the target, could be observed radiating around the target cell as Rtx-647 microclusters continued to accumulate at the base of the forming phagosome. Extension of the pseudopod followed, during which many microclusters were propelled forwarded over the target, suggesting that actin polymerization within the macrophage pseudopod propelled FcγR bound Rtx-647 over the target and resulted in a more uniform distribution of microclusters, over the internalized target, with a residual enrichment evident at the base of the phagosome (Fig 1B). These behaviors were consistent over 12 confocal and 3 LLSM movies. Taken together, these data indicate the macrophage drives rearrangement of Rtx in two phases, first an accumulation at the base of the phagocytic cup and second engulfment phase in which these microclusters are redistributed over the targe cell. In contrast to prior observations using macrophage-like RAW264.7 cells, which nearly exclusively perform trogocytosis of anti-CD20 IgG (Pham et al., 2011), most interactions resulted in complete ADCP. A small fraction (10-15%) of the anti-CD20 was removed into small vesicles prior to and during engulfment.

To determine if the forces responsible for reorganizing the Rtx-647 were generated by the macrophage, we imaged the redistribution of IgG on mobile and immobile supported lipid bilayers on silica beads (SLB-SB). The mobility of SB-SLBs was validated by FRAP followed by TIRF imaging (Supplement Fig. 1A). Upon contact with SLB-SBs made with fluid POPC, AF647-IgG formed a patch at the contact site (Fig. 1C). Engulfment of the SLB-SB resulted in redistribution of the IgG-AF647, recapitulating the

overall movements observed for Rtx-647 on B cell targets (Fig. 1B,C). When SLBs were made from gel-phase/immobile DPPC, macrophages were able to internalize them, with only minor changes in the IgG distribution (Fig. 1D). These data indicate that forces from the macrophage reposition mobile surface-associated IgG, in two phases, first an accumulation at the base of the phagosome followed by a redistribution around the target during engulfment. While the SLB-SB system provides an attractive tool for manipulating IgG mobility and IgG density (Bakalar et al., 2018); however, FLM and BDMDs readily internalize SLB-SBs independent of IgG, whereas IgG is essential for ADCP. To eliminate this confounding effect, we focused our efforts on using more physiological B cell targets.

To determine if the forces responsible for reorganizing the anti-CD20-AF647 IgG were generated by the macrophage, we imaged the redistribution of IgG on mobile and immobile supported lipid bilayers on silica beads (SLB-SB). The mobility of SB-SLBs was validated by FRAP at TIRF field (Supplement Fig 1A). During their interaction with SLB-SBs made with fluid POPC, AF647 IgG was observed for a large patch at the contact site during formation of the cup that was rapidly redistributed during the pseudopod extension and closure of the phagosome, recapitulating much of the overall movements observed for anti-CD20-AF647 IgG on the B cell targets (Fig. 1C. When SLBs were made from gel-phase/immobile DPPC macrophages were able to internalize them, with only minor changes in the IgG distribution (Fig. 1D). Taken together, these data indicate that forces from the forming phagosome will reposition surface associated IgG on targets that a fluid bilayer surface, but not surprisingly this repositioning is not required for ADCP. We originally had hoped that the SLB-SB system would be a useful

and easily manipulatable model for analyzing the impacts of surface mobility on ADCP as has been used in other studies (Bakalar et al., 2018), however, FLM and BDMDs readily internalize SLB-SBs independent of IgG, indicating that they behave quite differently than physiologically relevant ADCP targets.

Mobility of CD20/anti-CD20 on Wil2-s cells promotes ADCP

To determine the impact of IgG mobility on the target surface on the efficiency of ADCP, we manipulated the cytoskeleton of Wil2s cells and quantified ADCP as a function of anti-CD20-IgG density. To control for changes in the cell surface abundance of CD20 under these treatments, anit-CD20-AF647 IgG density was measured by flow cytometry and normalized (Supplement Fig. 1B). Treatment of cells with the actin depolymerizing drug, Latrunculin B (Lat B), imparted free diffusion to anti-CD20-IgG (Fig 2 C, D) and increased the sensitivity and phagocytic capacity of the ADCP response (Fig 2 A, C) over non-treated targets. In contrast, stabilization of the cytoskeleton while preserving the cell surface topography with the combination Jasplakinolide and Blebbistatin (Jas/Bleb) (Lou, Low-Nam, Kerkvliet, & Hoppe, 2014) had no discernable effect on ADCP over non-treated cells (Fig 2 C, D). Fixation of Wil2s cells with paraformaldehyde (PFA), to rigidify and immobilize the CD20 antigen impaired ADCP, indicating that the more mobile the anti-CD20-IgG, the more sensitive ADCP was to lower IgG concentrations (Fig 2 A-D). FRAP measurements of anti-CD20-AF647 IgG demonstrated that in both non-treated and Jas/Bleb treatments, that there was effectively no free diffusion (mobile fraction < 10%, Fig 2C) whereas treatment with Lat B resulted in free diffusion (mobile fraction > 67%, Fig. 2C), indicating that the Wil2s actin cytoskeleton restricted diffusion of anti-CD20-IgG. LLSM and confocal imaging of the anti-CD20-AF647 IgG during

ADCP illustrated pronounced microclustering and redistribution of anti-CD20-IgG was observed in the case of Lat B treated Wil2s cells (Fig. 1E, F), when compared with non-treated Wil2s targets (Fig. 1A and D), indicating that the forces generated by macrophage FcγRs can overcome diffusional restrictions on CD20 arising from the Wil2s cytoskeleton. Moreover, the increased patching of the anti-CD20-AF647 IgG in the case of LatB treated Wil2s cells lead to dramatic and intense recruitment of mScarlet-Syk. Analysis of ADCP in the context of PFA-treated Wil2s cells indicated that minimal rearrangement of anti-CD20-AF647 IgG was observed (Fig. 2 G-H), and far less Syk-mScarlet recruitment in both the LLSM example of failed ADCP (Fig. 2G) and low levels of recruitment in successful ADCP (Fig. 2H). Together, these findings indicate that microclustering, followed by patching of anti-CD20-IgG-FcγR complexes, driven by forces originating from the macrophage, are an important step in amplifying FcγR signaling, the recruitment of Syk and successful ADCP.

IgG surface mobility controls the topography of the macrophage-target interface and the distribution two populations of IgG-FcγR microclusters.

Given the potent enhancement of ADCP by increasing the mobility of the surface associated anti-CD20-IgG and the changes observed in the movements of anti-CD20-IgG/FcγR microclusters in response to targets displaying varying surface mobilities, we sought to capture a high-resolution view of the movements of membranes and anti-CD20-IgG/FcγR microclusters using our previously established TIRF microscopy methods (J. Lin et al., 2016). Here, SLBs on glass coverslips displaying AF-647 anti-biotin mIgG2a were created with POPC or DPPC lipids. FRAP confirmed that the POPC was fluid and mobile with a diffusion coefficient for the anti-biotin-IgG-AF647 of ~ 5 um^2/s (Fig. 3A,

B). Dropping DiI labeled FLM macrophages onto these surfaces and imaging by TIRF microscopy provided an exquisite view of the distribution of the plasma membrane and the movements of the anti-biotin-IgG-AF647. Consistent with our previous observations, interaction of the macrophage with mobile IgG resulted in the formation of focused IgG microclusters that transitioned into rapidly advancing lamellar sheets studded with small IgG microclusters (Fig. 3C). A fraction of these micrcoclusters would aggregate together and detach from the leading edge and move centripetally toward the center of the macrophage contact site, closely mirroring the movements of anti-CD20 IgG microclusters observed in confocal and LLS microscopies. Moreover, the use of the DiI signal afforded visualization of the membrane contact topography, where regions of DiI labeled macrophage membrane near the glass surface and within the ~100 nm illumination field of the TIRF microscope are brightly fluorescent. Furthermore, regions of the macrophage membrane that are far from the glass surface are not illuminated by the TIRF field and are dim/dark. By comparing the distribution of anti-biotin-IgG2a-AF647 to the DiI signal it was apparent that the IgG microclusteres were either restricted to the very tips of the advancing pseudopod which was generally followed by a bright region of DiI labeled plasma membrane, or in larger aggregated microclusters that generally moved toward the center of the cell and coincident with patches of DiI labeled plasma membrane within the TIRF field, and most plasma membrane was far from the glass reflecting either the distribution of tall proteins that supported it above the glass or from membrane tension created by actin tethers experiencing a contractile force. To gain a better understanding of the membrane topography, we applied Polarized-TIRF microscopy which is highly sensitive to changes in the topography of the plasma

membrane (Brandon, et al). Polarized-TIRF fields that were parallel (s-pol, S) or perpendicular (p-pol, P) to the coverslip were used to selectively excite Di I molecules in vertical or horizontal membrane. The ratio of P/S fluorescence images from DiI was used to encode membrane topography (Fig. 3E). Enlarged images of the leading edge shows that IgG microclusters were formed at where the P/S ratio was low, whereas areas with high P/S ratio had no IgG microclusters (Fig. 3F). This phenomenon can be seen quantitatively on the line scan graphs across the leading edge and a microcluster. The location of the leading edge and a microcluster were marked using white squares and white lines (Fig. 3F). Line scan across the leading edge showed the similar trend that IgG and PM intensities were in contrast with P/S ratio (Fig. 3H). Line scan across a microcluster also showed maximum IgG and PM intensities at the point where P/S ratio was the lowest (Fig. 3G). This topography was in stark contrast with the flat, radially expanding distribution of plasma membrane observed during engagement of IgG displayed on immobile SLB (Fig. 3D). Moreover, macrophages rearrange IgG/FcγR microclusters to the center of the contact site after stop spreading (Supplemental Fig. 2). This phenomenon is consistent with microclustering on wil2-s cells during ADCP which shows coupling of IgG/FcγR microclusters formation and actin-driven microcluster rearrangement.

Functional actin activity via Syk and Akt PH signaling triggered by IgG-FcγR microclusters is required for engaging on targets

The topography of the leading edge in which the microclusters form and the podosome-like patches of anti-CD20-IgG strongly suggest a role for the branched actin and its

remodeling in shaping of these FcγR signaling domains. Podosome is a protrusive actin-rich structure which is surrounded by a ring rich of adaptive proteins (Linder & Wiesner, 2015). To delineate how IgG mobility and Arp2/3 mediated actin branching contribute to IgG-FcγR signaling at microclusters and patches, we examined the recruitment of mScarlet-Syk as a measure of FcγR-ITAM activation and AktPH as a measure of PI3K activity while manipulating IgG mobility and Arp2/3 function. FLMs expressing mScarlet-Syk or mScarlet-AktPH were dropped onto anti-biotin-IgG-AF647 SLBs and imaging by TIRF microscopy. Similar to the confocal and LLSM imaging of ADCP, FLM on mobile POPC bilayers formed microclusters at the leading edge, that recruited mScarlet-Syk, and were then grouped into patches, the format of focused IgG microclusters that colocalized with Syk microclusters (Fig. 4A). Syk and IgG microclusters were rearranged together at the leading edge and move to the center of the macrophage contact site. Whereas interaction of the macrophage with immobile IgG resulted in no microcluter formation although the macrophage could still form the leading edge (Fig. 4B). The significance of actin signal amplification was further investigated by using FLMs expressing mScarlet-Akt PH. Consistent with Syk microcluster movement during interaction between FLMs and mobile IgG, Akt PH microclusters colocalized with IgG microclusters (Fig. 4 C).

CK666, a potent inhibitor of FLMs to investigate the importance of functional actin amplification during interaction with targets. Interestingly, FLMs could still form Akt PH microclusters, while no IgG microclusters were formed during engagement on immobile IgG (Fig. 4 D). Striking, we observed that the difference in diameters to which the cells

spread, with mobile POPC bilayers promoting macrophage spreading diameters that were ~125% larger than their counterparts spreading on DPPC bilayers (Fig. 4 G). As it was clear that Akt PH signal was amplified during engagement, FLMs were treated with CK 666 to inhibit actin activity. Indeed, CK 666 treated FLMs were not able to form the leading edge and spread while they were able to form IgG and Syk microclusters during engagement on a mobile/fluid POPC SLB (Fig. 4 E). During engagement on a immobile/gel-phase DPPC SLB, CK 666 treated FLMs tiptoed on the surface with no active spreading (Fig 4 F). The spreading area measurement on CK 666 treated FLMs showed 10 to 15 times less spreading than normal FLMs on SLBs constructed with mobile/fluid POPC and immobile/gel-phase DPPC (Fig. 4 G). CK 666 treatment on FLMs also significantly inhibited ADCP against Wil2s B cells opsonized with anti-CD20 AF 647 IgG. Anti-CD20 IgG microclusters formed, however, they stayed at the base of phagocytic cup which triggered IgG microcluster engulfment instead of ADCP (Fig. 4 H).

Successful ADCP depends on phagocytic signaling based on rearrangement of IgG/FcγR

Colocalization of IgG/FcγR microclusters with Syk and Akt PH near the leading edge and podosome-like patches during interaction with mobile/fluid SLBs suggest that Syk bound FcγR-ITAM signaling activates PI3K signal for phagocytic response. Also, suppressed spreading and the leading edge formation after CK 666 treatment during engagement on SLBs suggest overall phagocytic process depends on actin. However, failed phagocytosis examples showed that IgG/FcγR microcluster rearrangement is crucial. During failed phagocytosis on non-treated Wil2s B cells opsonized with the anti-CD20-AF647 IgG,

IgG/FcγR microclusters were stayed at the base of phagocytic cup as big patches which colocalized with Syk (Fig. 5A). Increased the anti-CD20-AF647 IgG patching on Lat B treated Wil2s B cells also triggered IgG/FcγR engulfment with Syk (Fig. 5B). Another failed phagocytosis by a Syk KO FLM taken from LLSM also showed that anti-CD20-AF647 IgG patches on a Wil2s B cell staying at the base of phagocytic cup which engulfed IgG/FcγR patches (Fig. 5C). These observations suggested that macrophages can still form microclusters without Syk, but ADCP requires proper Syk and IgG/FcγR rearrangement. Such phenomenon looked similar to trogocytosis which is an immune respone of nibbling on pathogens (Guillen, 2014). To investigate if engulfment of IgG/FcγR patches involve nibbling of cell body, we challenged FLMs by Wil2s B cells expressing mScarlet-Mem opsonized with anti-CD20-AF647 IgG. Indeed, a big IgG/FcγR patch was engulfed with a chunk of Wil2s B cell body (Fig. 5D). All these observations showed that IgG/FcγR and Syk microclutsering occurs even when macrophages fail phagocytosis. However, proper Syk and Arp 2/3 activities are required to rearrange IgG/FcγR microclusters near the leading edge and to limit trogocytosis.

Discussion

The antigen mobility on the target surface provided new insight into the IgG/FcγR microclusters that must be engaged and rearranged for triggering efficient ADCP. Traditionally, zipper model posits the sequential FcγR engagement on IgG during ADCP, while trigger model posits sufficient FcγR binding to IgGs to activate phagocytic signal (Griffin et al., 1975; Griffin et al., 1976). Our findings give understanding that not only IgG/FcγR microcluster formation but also proper IgG/FcγR microcluster rearrangement for phagocytic signal amplification is required to trigger ADCP.

Specifically, we found that changing CD20 mobility on WIL2-S B cells using Lat B treatment enhanced sensitivity to ADCP, whereas rigidifying WIL2-S B cells with PFA treatement suppressed ADCP (Fig. 2 A-D). Confocal and LLSM imaging showed that IgG/FcγR microclusters rearrangement colocalizing with Syk during ADCP of no drug treated WIL2-S cells (Fig. 1 A, B). This phenomenon is more dynamic on Lat B treated WIL2-S B cells with forming bigger patches (Fig. 2 E, F). However, IgG and Syk microclusters were not formed during engagement on PFA treated WIL2-S cells (Fig. 2 G,H). IgG microclustering behavior was consistent on opsonized SLB-SBs constructed by mobile/fluid POPC and immobile/gel-phase DPPC. During ADCP of SLB-SBs, patches were formed on the surface of a mobile/fluid POPC SLB-SB which was not seen on a immobile/gel-phase DPPC SLB-SB (Fig. 1 C,D). These observations show that lack of IgG/FcγR microclusters on targets with perfectly immobile antigens lead to less phagocytic response. During ADCP on targets with mobile antigens, IgG/FcγR microclusters are formed and rearranged which result in better phagocytic response. However, failed phagocytosis examples showed that proper microcluster rearrangement is required to trigger ADCP. During failed phagocytosis, IgG/FcγR microclusters stayed at the base of phagocytic cup which triggered trogocytosis. Confocal imaging on no drug treated WIL2-S B cells during failed phagocytosis showed big IgG and Syk patches formed and colocalized to each other; however, they stayed at the base of phagocytic cup (Fig. 5 A). This phenomenon was more obvious during failed phagocytosis on Lat B treated WIL2-S B cells which had bigger IgG and Syk patches formed and colocalized to each other (Fig. 5 B). Insterestingly, lack of Syk also induced a similar IgG patches at the base of phagocytic cup during LLSM imaging (Fig. 5 C). This suggests that IgG

microclusters can be formed even without Syk, but Syk is required for proper IgG rearrangement during ADCP. During IgG engulfment, a chunk of target cell body is also engulfed (Fig. 5 D). This suggests the importance of moderate phagocytic signal across the phagocytic cup to trigger ADCP rather than triggering high phagocytic signal at the base of the phagocytic cup. These results could be explained by combining both zipper model and trigger model. For successful ADCP, FcγRs sequentially engage on IgGs on the target surface forming IgG/FcγR microclusters which amplifies Syk and Arp 2/3 signaling as IgG/FcγR microclusters are rearranged; IgG/FcγR microclusters are propelled forwared as membrane is extended around the target which fully engulf the target at the end (Fig. 6). For failed ADCP, initial IgG/FcγR microcluster formation is similar to successful ADCP; however, IgG/FcγR microclusters stay at the base of phagocytic cup as big patches; This amplifies phagocytic signal concentrated at the base of phagocytic cup which results in engulfing IgG/FcγR microclusters before membrane extension (Fig. 6).

The overall result from WIL2-S cell ADCP was consistent with experiments using mobile/fluid and immobile/gel-phase SLBs. Macrophages were able to form the leading edge and IgG/FcγR microclusters (Fig. 3 C) colocalizing with Syk and Akt PH during engagement on opsonized mobile/fluid SLBs (Fig. 4 A, C). However, IgG/FcγR microclusters colocalizing with Syk and Akt PH were not formed while engaging on immobile/gel-phase SLBs (Fig. 3 D and 4 B, D). Other than forming IgG/FcγR microclusters, membrane topography was significantly different between engagement on mobile/fluid and immobile/gel-phase SLBs. Imaging at TIRF field showed the signal from lipophilic dye on FLMs had almost no difference across the membrane at the

contact site with immobile/gel-phase SLBs (Fig. 3 D). Evanescent field created at TIRF field only involves the fluorescent signal 100 nm apart from the source which allows to only capture fluorescent signal close to the contact site. TIRF imaging during engagement on mobile/fluid SLBs showed a flower-like pattern from anti-Biotin AF 647 mIgG2a on SLBs and lipophilic dye from macrophages at the contact site. The pattern showed regions with bright PM signal including the leading edge and the center of the contact site colocalize with IgG microclusters (Fig. 3 C). The membrane topography is further studied using pol-TIRF imaging that showed overall spatial orientation and membrane dynamics during engagement on fluid bilayers (Fig. 3E). Pol-TIRF imaging clearly showed macrophages forming the leading edge and podosome-like structures around IgG/FcγR microclusters (Fig. 3F). The line scanning across the leading edge and podosome-like structure (marked with white line on Fig. 3F) gave better insight on membrane dynamics. Quantified signal across both the leading edge and a posome-like structure showed high P/S ratio before and after high IgG and PM signals (Fig. 3 G, H). Presumably, macrophages would form the actin rich structure surrounding IgG/FcγR microclusters perpendicular to the surface. Together, these observations indicate that there are many parallels across IgG/FcγR immune complex that microclustering and actin-driven rearrangement of IgG/FcγR is a common theme on both ADCP against phagocytic targets and engagement on SLBs.

These findings challenge the old observation that a uniform distribution of IgG is important for ADCP. However, the support the notion that clustering of the FcγRs are an important step in signal amplification for ADCP. Moreover, when combined with the data from figure 1, it is clear that the macrophage cytoskeleton provides the driving force

for clustering and moving the anti-CD20-IgG. TIRF data on CK 666 treated FLMs from figure 4 strengthen that macrophage cytoskeleton plays an important role for clustering and moving IgG.

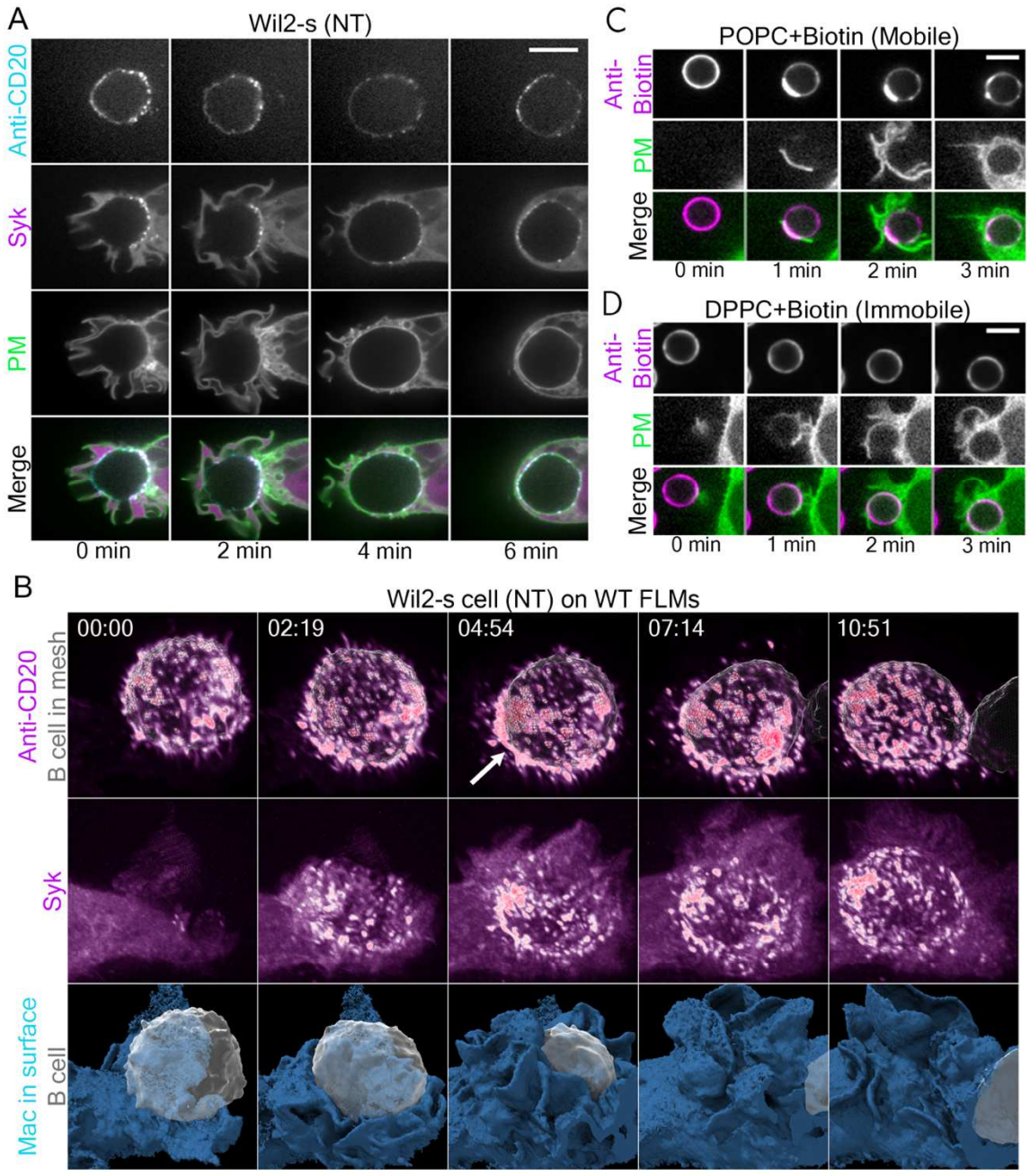

Figure 2.1 IgG microcluster formation and Syk recruitment and redistribution during ADCP. (**A**) Confocal imaging of ADCP of WIL2-S cells opsonized with Rtx-647

by FLMs expressing Mem-mNG (PM) and Syk-mScarlet. Syk and Rtx-647 form microclusters and colocalize to each other at the contact site. During engulfment, microclusters redistribute over the target surface (scale bar = 10 μm). (**B**) LLSM imaging of ADCP of WIL2-S cells labeled with calcein violet and opsonized with Rtx-647 by an FLM expressing Mem-mNG and Syk-mScarlet. During cup formation, microclusters pooled into patches (arrow) at the base of the phagocytic cup. As engulfment proceeded, the microclusters bearing Syk-mScarlet were redistributed over the surface of the B cell (Image dimension = 20 μm x 20 μm). mIgG2a-AF647 displayed on SLBs on silica beads pooled at the base of the phagosome formed by PKH67-labeled FLMs and then redistributed over the bead when presented on fluid POPC (**C**) but not gel-phase/immobile DPPC (**D**) SLBs (scale bar = 5 μm).

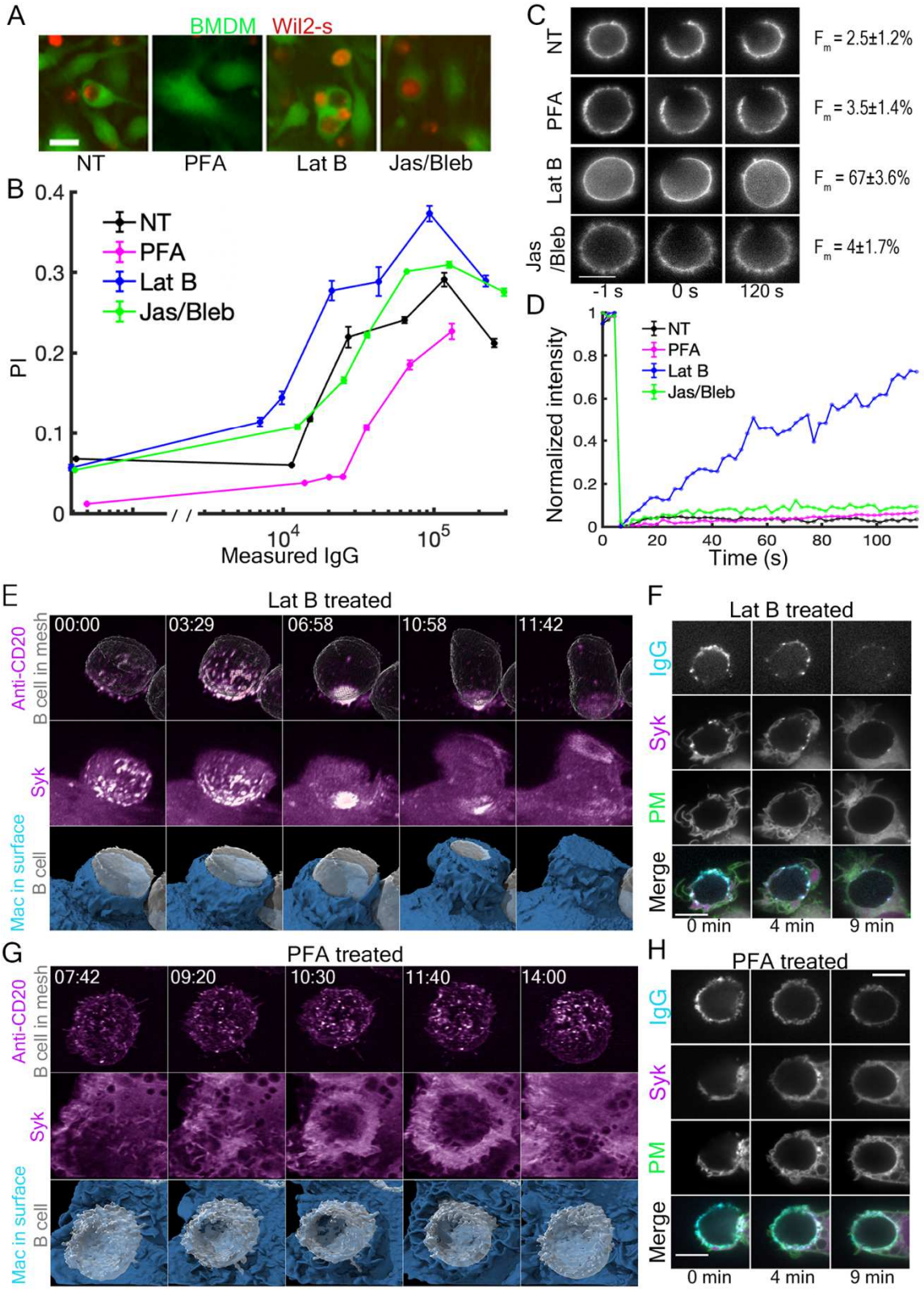

Figure 2.2 Enhanced ADCP and IgG/Syk microcluster rearrangement with increasing CD20 mobility. (**A**) High content imaging of BMDMs (green) and internalized WIL2-S cells (pHrodoRed) opsonized with Rtx following manipulation of

actin (NT, PFA, Lat B and Jas/bleb, scale bar = 10μm). (**B**) Quantified phagocytic index (PI) for measured Rtx(IgG) densities on WIL2-S cells that were untreated or pretreated with Lat B, Jas/Bleb or PFA (error bars are standard error of the mean, n = 2 experiments). (**C** and **D**) FRAP images and normalized recovery traces of Rtx-647 on single WIL2-S cells treated with different actin disrupting drugs, (average mobile fraction (F_M) for 10 cells per condition, error is std. dev., scale bar = 10 μm). No recovery of Rtx-647 on WIL2-S cells treated with no drug, PFA and Jas/Bleb. LLSM of calcein violet labeled WIL2-S cells opsonized with Rtx-647 and pretreated with Lat B during complete ADCP (**E**) or PFA during failed ADCP (**G**) by FLMs expressing Mem-mNG and mScarlet-Syk. For the Lat B treatment, Rtx-647 microclusters and patches accumulated at the base of WIL2-S/FLM contact site and intensely recruited Syk-mScarlet and then redistributed to near uniformity during engulfment. Minimal rearrangement of Rtx-647 occurred on PFA treated WIL2-S cells (image dimension = 21 μm x 21 μm for E and 25 μm x 25 μm for G). Confocal imaging during complete ADCP of WIL2-S cells treated with Lat B (**F**) or PFA (**H**, scale bar = 10 μm).

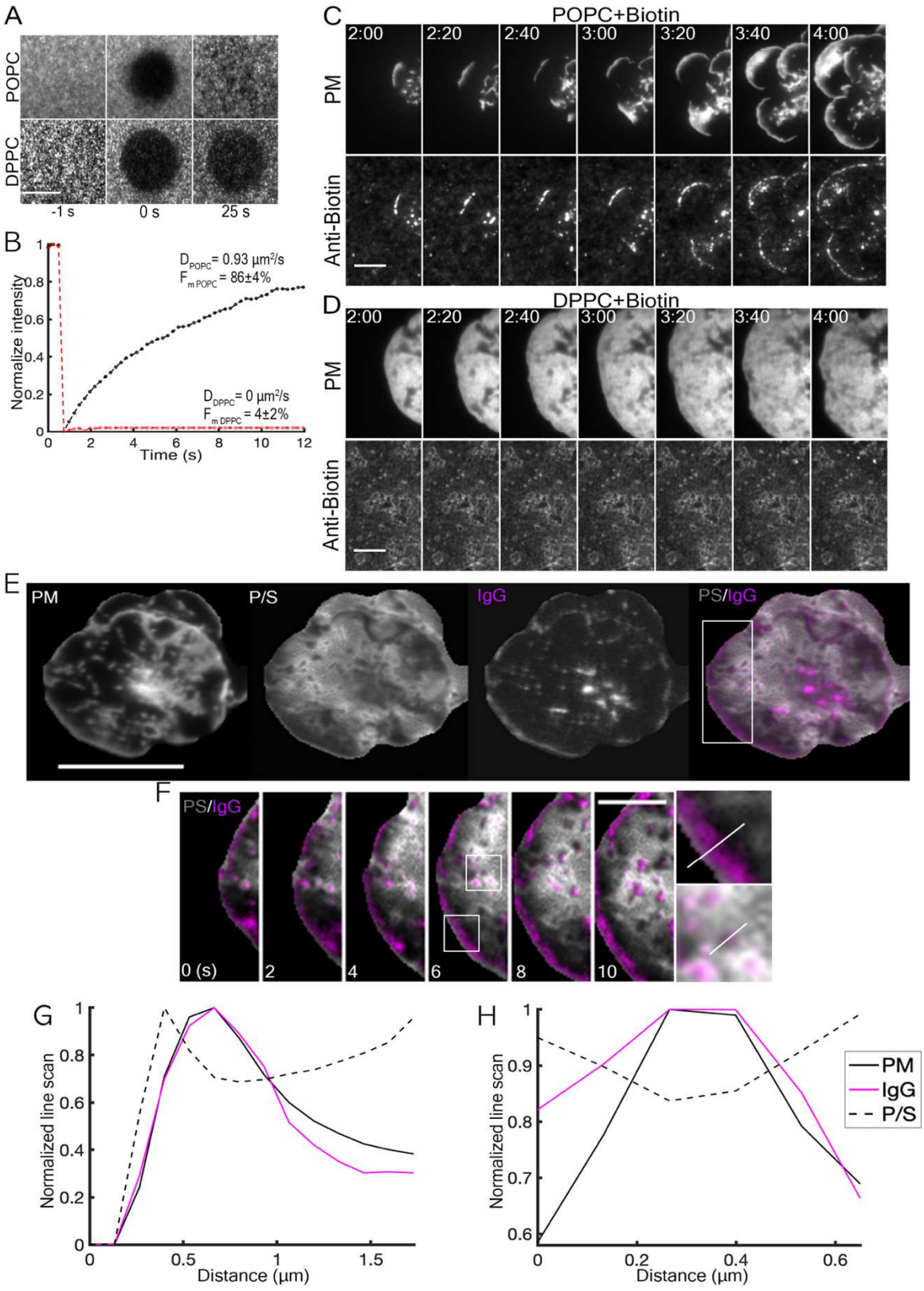

Figure 2.3 Imaging of IgG microcluster dynamics and membrane topography on fluid and immobile SLBs. (**A**) TIRF-FRAP of IgG-AF647 presented on mobile/fluid POPC or

gel-phase/immobile DPPC SLBs. (**B**) IgG-AF647 on POPC SLBs displayed rapid diffusion with a high mobile fraction, whereas IgG-AF647 were immobile. TIRF imaging of IgG-AF647 relative to the FLM plasma membrane (labeled with DiI) during engagement on mobile/fluid POPC (**C**) or gel-phase/immobile DPPC (**D**) SLBs (scale bar = 5 μm). (**E**) Pol-TIRF imaging of an FLM labeled with DiI on relative to mobile IgG-AF647 presented on fluid POPC SLB. PM is the total DiI signal (P+2S), and membrane curvature is observed in the P/S ratio (high intensity = vertical membrane, low intensity = flat) relative to IgG-AF647 microclusters (magenta) (scale bar = 10 μm). (**F**) A zoomed region of the leading edge illustrates IgG-AF647 movements during pseudopod advancement and development of podosome-like structures which are enlarged on the right (scale bar = 5 μm). Line scan of the leading edge (**G**) illustrates, high P/S at the tip, followed by an intense band of PM, note that the PM signal and increase in P/S persists on the trailing side of the IgG-AF647 curve. Line scan across a podosome-like structure (**H**), indicated maximal IgG-AF647 signal on a flat patch of PM and surrounded by vertical membrane (high P/S).

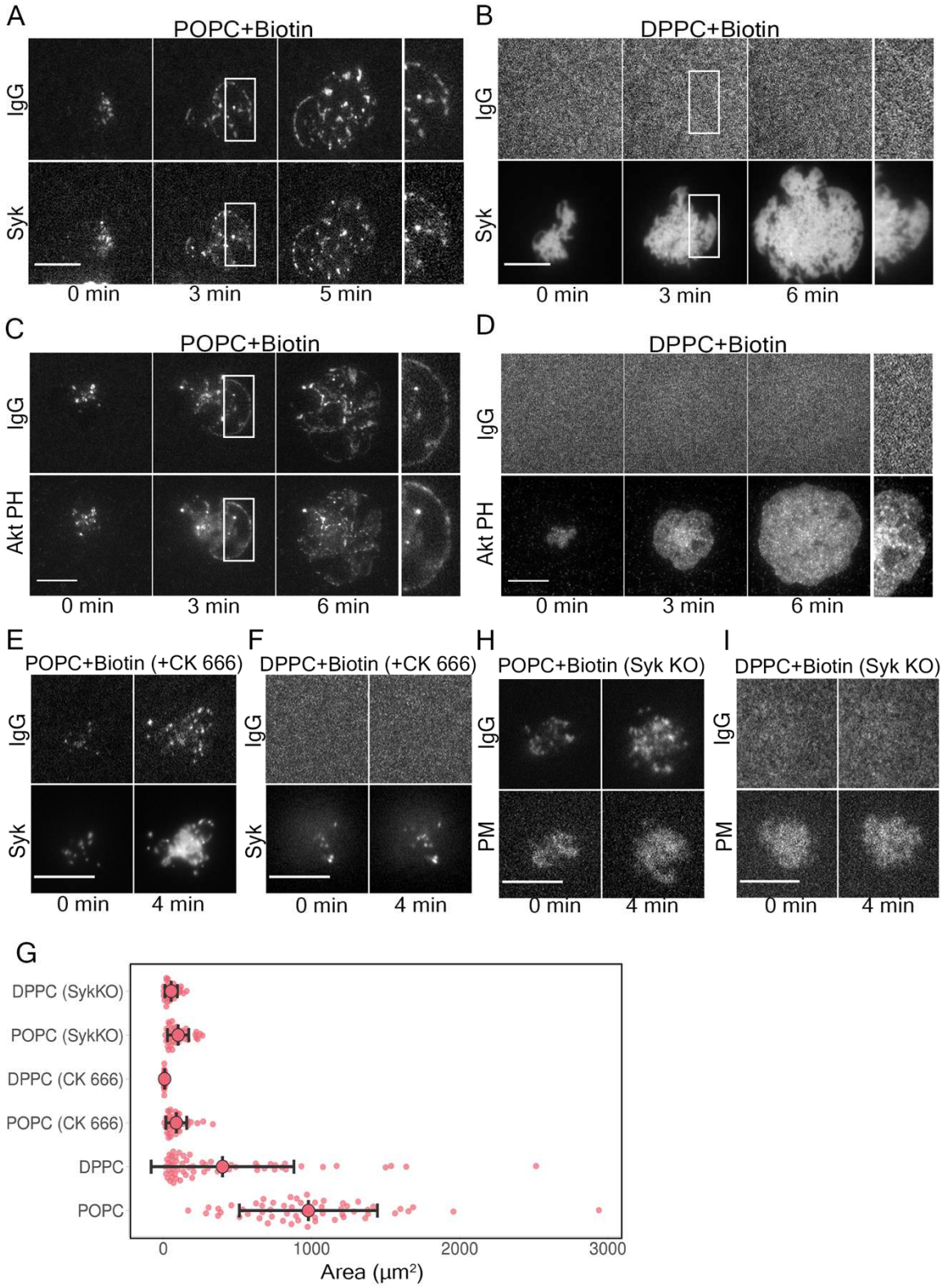

Figure 2.4 Syk and PI3K signaling originates from IgG microclusters and is supported by an Arp2/3-Syk amplification loop. (**A-B**) TIRF imaging of FLMs expressing Syk-mScarlet on IgG-AF647 presenting mobile/fluid POPC or gel-

phase/immobile DPPC SLBs (scale bar = 10 μm). (**C-D**) AktPH-mScarlet was used to visualize the PI3K products in FLM cells engaging IgG-AF647 presented on POPC or DPPC bilayers (scale bar = 10 μm). (**E-F**) IgG-AF647 distribution and Syk-mScarlet localization on POPC or DPPC bilayers engaged by CK 666 treated FLM cells expressing Mem-mNG (scale bar = 10 μm). (**G-H**) Distribution of IgG-AF647 presented on POPC or DPPC bilayers engaged by Syk KO FLM cells bearing Mem-mNG. (**G)** Quantification of FLM cell spreading across the conditions above. Normal FLMs were able to spread on mobile/fluid SLBs better than on immobile/gel-phase SLBs overall. Syk KO and CK 666 treated FLMs were defective in cell spreading, while they could spread better on mobile/fluid SLBs than immobile/gel-phase SLBs.

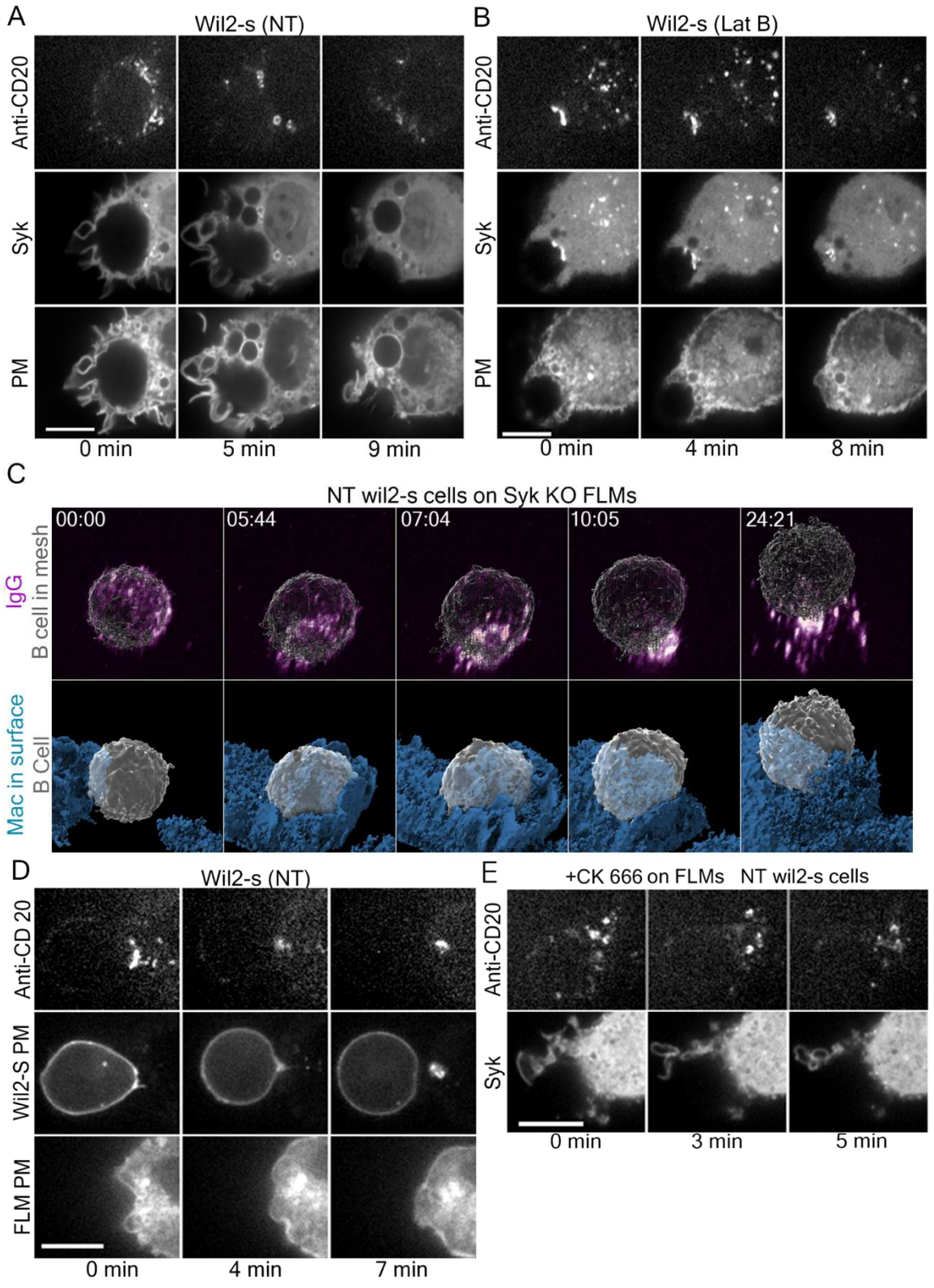

Figure 2.5 Syk and Arp2/3 mediate IgG rearrangement, promote ADCP and limits trogocytic clearance of anti-CD20 from B lymphoma targets. Confocal imaging of

trogocytosis on WIL2-S B cells treated with no drug (**A**) and Lat B (**B**). WIL2-S cells were also opsonized with Rtx-647. During trogocytosis by FLMs expressing Mem-mNG and Syk-mScarlet, Syk and Rtx-647 microclusters colocalize to each other at the contact site and exist as patches at the base of phagocytic cup (scale bar = 10 μm). (**C**) LLSM imaging of trogocytosis of WIL2-S cells labeled with calcein violet and opsonized with Rtx-647 by a Syk KO FLM expressing Mem-mNG. Rtx-647 forms microclusters and exist as a big patch at the base of phagocytic cup (Image dimension = 20 μm x 20 μm). (**D**) Confocal imaging of trogocytosis on WIL2-S B cells expressing Mem-mScarlet and opsonized with Rtx-647. During trogocytosis by FLMs expressing Mem-mNG, Rtx-647 microclusters from a big patch at the base of phagocytic cup. Small portion of WIL2-S cell plasma membrane is taken off with Rtx-647 (scale bar = 10 μm). **(E)** Confocal imaging of trogocytosis on WIL2-S B cells expressing Mem-mScarlet and opsonized with Rtx-647 (scale bar = 10 μm).

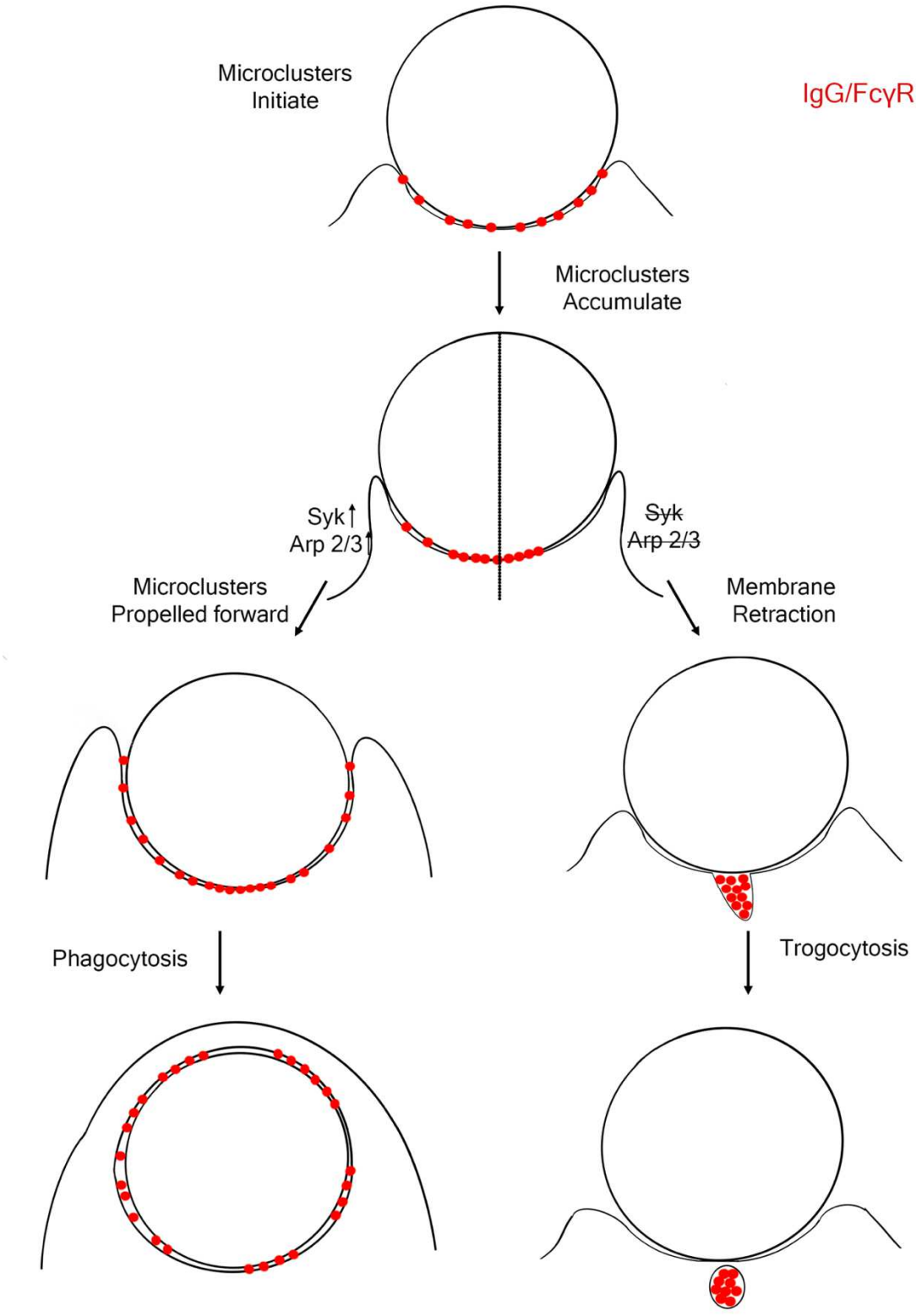

Figure 6. ADCP and trogocytosis are dependent on IgG/FcγR microclusters rearrangement at the contact site. Pictorial diagram of ADCP and trogocytosis process by macrophages against phagocytic targets showing IgG/FcγR microcluster movement

represented by small red circles. IgG/FcγR microclusters formation is common theme for both ADCP and trogocytosis. During ADCP, IgG/FcγR microclusters are formed at the base of phagocytic cup and propelled forward with the leading edge. Syk and Arp2/3 signals are amplified across the phagocytic cup. During trogocytosis, IgG/FcγR microclusters exist as big patches at the base of phagocytic cup without rearrangement. Syk and Arp2/3 signals are concentrated at the base of phagocytic cup which induce nibbling of IgG/FcγR microclusters.

Reference

Ackerman, M. E., Dugast, A. S., McAndrew, E. G., Tsoukas, S., Licht, A. F., Irvine, D. J., & Alter, G. (2013). Enhanced phagocytic activity of HIV-specific antibodies correlates with natural production of immunoglobulins with skewed affinity for FcgammaR2a and FcgammaR2b. *J Virol, 87*(10), 5468-5476. doi:10.1128/JVI.03403-12

Alvey, C., & Discher, D. E. (2017). Engineering macrophages to eat cancer: from "marker of self" CD47 and phagocytosis to differentiation. *J Leukoc Biol, 102*(1), 31-40. doi:10.1189/jlb.4RI1216-516R

Alvey, C. M., Spinler, K. R., Irianto, J., Pfeifer, C. R., Hayes, B., Xia, Y., . . . Discher, D. E. (2017). SIRPA-Inhibited, Marrow-Derived Macrophages Engorge, Accumulate, and Differentiate in Antibody-Targeted Regression of Solid Tumors. *Curr Biol, 27*(14), 2065-2077 e2066. doi:10.1016/j.cub.2017.06.005

Bailey, E. M., Choudhury, A., Vuppula, H., Ortiz, D., Schaeck, J., Manning, A. M., . . . Hoppe, A. D. (2020). Engineered IgG1-Fc molecules define valency control of cell surface Fcg receptor inhibition and activation in endosomes. doi:10.3389/fimmu.2020.617767

Bakalar, M. H., Joffe, A. M., Schmid, E. M., Son, S., Podolski, M., & Fletcher, D. A. (2018). Size-Dependent Segregation Controls Macrophage Phagocytosis of Antibody-Opsonized Targets. *Cell, 174*(1), 131-142 e113. doi:10.1016/j.cell.2018.05.059

Barkal, A. A., Weiskopf, K., Kao, K. S., Gordon, S. R., Rosental, B., Yiu, Y. Y., . . . Maute, R. L. (2018). Engagement of MHC class I by the inhibitory receptor LILRB1 suppresses macrophages and is a target of cancer immunotherapy. *Nat Immunol, 19*(1), 76-84. doi:10.1038/s41590-017-0004-z

Boross, P., Jansen, J. H., de Haij, S., Beurskens, F. J., van der Poel, C. E., Bevaart, L., . . . Leusen, J. H. (2011). The in vivo mechanism of action of CD20 monoclonal antibodies depends on local tumor burden. *Haematologica, 96*(12), 1822-1830. doi:10.3324/haematol.2011.047159

Boudreau, C. M., & Alter, G. (2019). Extra-Neutralizing FcR-Mediated Antibody Functions for a Universal Influenza Vaccine. *Front Immunol, 10*, 440. doi:10.3389/fimmu.2019.00440

Brandsma, A. M., Schwartz, S. L., Wester, M. J., Valley, C. C., Blezer, G. L. A., Vidarsson, G., . . . Leusen, J. H. W. (2018). Mechanisms of inside-out signaling of the high-affinity IgG receptor FcgammaRI. *Sci Signal, 11*(540). doi:10.1126/scisignal.aaq0891

Chao, M. P., Alizadeh, A. A., Tang, C., Myklebust, J. H., Varghese, B., Gill, S., . . . Majeti, R. (2010). Anti-CD47 antibody synergizes with rituximab to promote phagocytosis and eradicate non-Hodgkin lymphoma. *Cell, 142*(5), 699-713. doi:10.1016/j.cell.2010.07.044

Chen, B. C., Legant, W. R., Wang, K., Shao, L., Milkie, D. E., Davidson, M. W., . . . Betzig, E. (2014). Lattice light-sheet microscopy: imaging molecules to embryos at high spatiotemporal resolution. *Science, 346*(6208), 1257998. doi:10.1126/science.1257998

Church, A. K., VanDerMeid, K. R., Baig, N. A., Baran, A. M., Witzig, T. E., Nowakowski, G. S., & Zent, C. S. (2016). Anti-CD20 monoclonal antibody-dependent phagocytosis of chronic lymphocytic leukaemia cells by autologous macrophages. *Clin Exp Immunol, 183*(1), 90-101. doi:10.1111/cei.12697

Dahal, L. N., Dou, L., Hussain, K., Liu, R., Earley, A., Cox, K. L., . . . Beers, S. A. (2017). STING Activation Reverses Lymphoma-Mediated Resistance to Antibody Immunotherapy. *Cancer Res, 77*(13), 3619-3631. doi:10.1158/0008-5472.CAN-16-2784

Dahal, L. N., Huang, C. Y., Stopforth, R. J., Mead, A., Chan, K., Bowater, J. X., . . . Beers, S. A. (2018). Shaving Is an Epiphenomenon of Type I and II Anti-CD20-Mediated Phagocytosis, whereas Antigenic Modulation Limits Type I Monoclonal Antibody Efficacy. *J Immunol, 201*(4), 1211-1221. doi:10.4049/jimmunol.1701122

Freeman, S. A., Goyette, J., Furuya, W., Woods, E. C., Bertozzi, C. R., Bergmeier, W., . . . Grinstein, S. (2016). Integrins Form an Expanding Diffusional Barrier that Coordinates Phagocytosis. *Cell, 164*(1-2), 128-140. doi:10.1016/j.cell.2015.11.048

Gordan, S., Biburger, M., & Nimmerjahn, F. (2015). bIgG time for large eaters: monocytes and macrophages as effector and target cells of antibody-mediated immune activation and repression. *Immunol Rev, 268*(1), 52-65. doi:10.1111/imr.12347

Gordon, S. R., Maute, R. L., Dulken, B. W., Hutter, G., George, B. M., McCracken, M. N., . . . Weissman, I. L. (2017). PD-1 expression by tumour-associated macrophages inhibits phagocytosis and tumour immunity. *Nature, 545*(7655), 495-499. doi:10.1038/nature22396

Griffin, F. M., Jr., Griffin, J. A., Leider, J. E., & Silverstein, S. C. (1975). Studies on the mechanism of phagocytosis. I. Requirements for circumferential attachment of particle-bound ligands to specific receptors on the macrophage plasma membrane. *J Exp Med, 142*(5), 1263-1282. doi:10.1084/jem.142.5.1263

Griffin, F. M., Jr., Griffin, J. A., & Silverstein, S. C. (1976). Studies on the mechanism of phagocytosis. II. The interaction of macrophages with anti-immunoglobulin IgG-coated bone marrow-derived lymphocytes. *J Exp Med, 144*(3), 788-809. doi:10.1084/jem.144.3.788

Gul, N., & van Egmond, M. (2015). Antibody-Dependent Phagocytosis of Tumor Cells by Macrophages: A Potent Effector Mechanism of Monoclonal Antibody Therapy of Cancer. *Cancer Res, 75*(23), 5008-5013. doi:10.1158/0008-5472.CAN-15-1330

He, W., Chen, C. J., Mullarkey, C. E., Hamilton, J. R., Wong, C. K., Leon, P. E., . . . Tan, G. S. (2017). Alveolar macrophages are critical for broadly-reactive antibody-mediated protection against influenza A virus in mice. *Nat Commun, 8*(1), 846. doi:10.1038/s41467-017-00928-3

Jaumouille, V., Farkash, Y., Jaqaman, K., Das, R., Lowell, C. A., & Grinstein, S. (2014). Actin cytoskeleton reorganization by Syk regulates Fcgamma receptor responsiveness by increasing its lateral mobility and clustering. *Dev Cell, 29*(5), 534-546. doi:10.1016/j.devcel.2014.04.031

Lambert, T., & Shao, L. (2019). tlambert03/LLSpy: v0.4.8. doi:http://doi.org/10.5281/zenodo.3554482

Lin, J., Kurilova, S., Scott, B. L., Bosworth, E., Iverson, B. E., Bailey, E. M., & Hoppe, A. D. (2016). TIRF imaging of Fc gamma receptor microclusters dynamics and signaling on macrophages during frustrated phagocytosis. *BMC Immunol, 17*, 5. doi:10.1186/s12865-016-0143-2

Linder, S., & Wiesner, C. (2015). Tools of the trade: podosomes as multipurpose organelles of monocytic cells. *Cell Mol Life Sci, 72*(1), 121-135. doi:10.1007/s00018-014-1731-z

Lou, J., Low-Nam, S. T., Kerkvliet, J. G., & Hoppe, A. D. (2014). Delivery of CSF-1R to the lumen of macropinosomes promotes its destruction in macrophages. *J Cell Sci, 127*(Pt 24), 5228-5239. doi:10.1242/jcs.154393

Marshall, M. J. E., Stopforth, R. J., & Cragg, M. S. (2017). Therapeutic Antibodies: What Have We Learnt from Targeting CD20 and Where Are We Going? *Front Immunol, 8*, 1245. doi:10.3389/fimmu.2017.01245

Matlung, H. L., Babes, L., Zhao, X. W., van Houdt, M., Treffers, L. W., van Rees, D. J., . . . van den Berg, T. K. (2018). Neutrophils Kill Antibody-Opsonized Cancer Cells by Trogoptosis. *Cell Rep, 23*(13), 3946-3959 e3946. doi:10.1016/j.celrep.2018.05.082

McQuin, C., Goodman, A., Chernyshev, V., Kamentsky, L., Cimini, B. A., Karhohs, K. W., . . . Carpenter, A. E. (2018). CellProfiler 3.0: Next-generation image processing for biology. *PLoS Biol, 16*(7), e2005970. doi:10.1371/journal.pbio.2005970

Minard-Colin, V., Xiu, Y., Poe, J. C., Horikawa, M., Magro, C. M., Hamaguchi, Y., . . . Tedder, T. F. (2008). Lymphoma depletion during CD20 immunotherapy in mice is mediated by macrophage FcgammaRI, FcgammaRIII, and FcgammaRIV. *Blood, 112*(4), 1205-1213. doi:10.1182/blood-2008-01-135160

Morrissey, M. A., Williamson, A. P., Steinbach, A. M., Roberts, E. W., Kern, N., Headley, M. B., & Vale, R. D. (2018). Chimeric antigen receptors that trigger phagocytosis. *Elife, 7*. doi:10.7554/eLife.36688

Mullarkey, C. E., Bailey, M. J., Golubeva, D. A., Tan, G. S., Nachbagauer, R., He, W., . . . Palese, P. (2016). Broadly Neutralizing Hemagglutinin Stalk-Specific Antibodies Induce Potent Phagocytosis of Immune Complexes by Neutrophils in an Fc-Dependent Manner. *mBio, 7*(5). doi:10.1128/mBio.01624-16

Niedergang, F., Di Bartolo, V., & Alcover, A. (2016). Comparative Anatomy of Phagocytic and Immunological Synapses. *Front Immunol, 7*, 18. doi:10.3389/fimmu.2016.00018

Park, W. S., Heo, W. D., Whalen, J. H., O'Rourke, N. A., Bryan, H. M., Meyer, T., & Teruel, M. N. (2008). Comprehensive identification of PIP3-regulated PH domains from C. elegans to H. sapiens by model prediction and live imaging. *Mol Cell, 30*(3), 381-392. doi:10.1016/j.molcel.2008.04.008

Pham, T., Mero, P., & Booth, J. W. (2011). Dynamics of macrophage trogocytosis of rituximab-coated B cells. *PLoS One, 6*(1), e14498. doi:10.1371/journal.pone.0014498

Planchon, T. A., Gao, L., Milkie, D. E., Davidson, M. W., Galbraith, J. A., Galbraith, C. G., & Betzig, E. (2011). Rapid three-dimensional isotropic imaging of living cells using Bessel beam plane illumination. *Nat Methods, 8*(5), 417-423. doi:10.1038/nmeth.1586

Quinn, S. E., Huang, L., Kerkvliet, J. G., Swanson, J. A., Smith, S., Hoppe, A. D., . . . Scott, B. L. (2020). The structural dynamics of macropinosome formation and PI3-kinase-mediated sealing revealed by lattice light sheet microscopy. *BioRxiv*, 2020.2012.2001.390195. doi:10.1101/2020.12.01.390195

Rudnicka, D., Oszmiana, A., Finch, D. K., Strickland, I., Schofield, D. J., Lowe, D. C., . . . Davis, D. M. (2013). Rituximab causes a polarization of B cells that augments its therapeutic function in NK-cell-mediated antibody-dependent cellular cytotoxicity. *Blood, 121*(23), 4694-4702. doi:10.1182/blood-2013-02-482570

Schindelin, J., Arganda-Carreras, I., Frise, E., Kaynig, V., Longair, M., Pietzsch, T., . . . Cardona, A. (2012). Fiji: an open-source platform for biological-image analysis. *Nat Methods, 9*(7), 676-682. doi:10.1038/nmeth.2019

Scott, B. L., Sochacki, K. A., Low-Nam, S. T., Bailey, E. M., Luu, Q., Hor, A., . . . Hoppe, A. D. (2018). Membrane bending occurs at all stages of clathrin-coat assembly and defines endocytic dynamics. *Nature Communications, 9*. doi:ARTN 419

10.1038/s41467-018-02818-8

Shapouri-Moghaddam, A., Mohammadian, S., Vazini, H., Taghadosi, M., Esmaeili, S. A., Mardani, F., . . . Sahebkar, A. (2018). Macrophage plasticity, polarization, and function in health and disease. *J Cell Physiol, 233*(9), 6425-6440. doi:10.1002/jcp.26429

Sips, M., Krykbaeva, M., Diefenbach, T. J., Ghebremichael, M., Bowman, B. A., Dugast, A. S., . . . Alter, G. (2016). Fc receptor-mediated phagocytosis in tissues as a potent mechanism for preventive and therapeutic HIV vaccine strategies. *Mucosal Immunol, 9*(6), 1584-1595. doi:10.1038/mi.2016.12

Swanson, J. A., & Hoppe, A. D. (2004). The coordination of signaling during Fc receptor-mediated phagocytosis. *J Leukoc Biol, 76*(6), 1093-1103. doi:10.1189/jlb.0804439

Tsai, R. K., & Discher, D. E. (2008). Inhibition of "self" engulfment through deactivation of myosin-II at the phagocytic synapse between human cells. *J Cell Biol, 180*(5), 989-1003. doi:10.1083/jcb.200708043

Vaughan, A. T., Chan, C. H., Klein, C., Glennie, M. J., Beers, S. A., & Cragg, M. S. (2015). Activatory and inhibitory Fcgamma receptors augment rituximab-mediated internalization of CD20 independent of signaling via the cytoplasmic domain. *J Biol Chem, 290*(9), 5424-5437. doi:10.1074/jbc.M114.593806

Velmurugan, R., Challa, D. K., Ram, S., Ober, R. J., & Ward, E. S. (2016). Macrophage-Mediated Trogocytosis Leads to Death of Antibody-Opsonized Tumor Cells. *Mol Cancer Ther, 15*(8), 1879-1889. doi:10.1158/1535-7163.MCT-15-0335

Weiskopf, K., & Weissman, I. L. (2015). Macrophages are critical effectors of antibody therapies for cancer. *MAbs, 7*(2), 303-310. doi:10.1080/19420862.2015.1011450

CHAPTER III. DISCUSSION

Understanding the mechanisms of FcγR microclustering and signal transduction is an important goal for immunology and developing potent immunotherapies. In this thesis, the imaging of FcγR microclusters provided the enhanced understanding of the importance of antigen-antibody mobility and proper distribution of FcγR signals during ADCP.

The enhancement of ADCP by antigen-antibody mobility provides a new perspective for understanding how the molecular arrangement of FcγRs can influence the cellular immune response. This research showed that macrophages rearrange antigen-antibody complexes as they trigger phagocytic responses. Specifically, CD20 molecules bound with anti-CD20 antibodies on Wil2s B cells formed microclusters which are reorganized during phagocytic process. Manipulation of the target cell cytoskeleton changed the ability of macrophages to rearrange IgG-CD20. Depolymerization of the target cytoskeleton produced fully mobile IgG-CD20 and enhanced ADCP, whereas fixation of the cytoskeleton immobilized IgG-CD20 and suppressed ADCP. This effect was recapitulated on mobile/fluid and immobile/gel-phase SLBs where macrophages were made to observe IgG microclustering event during engagement using TIRF imaging. Biotin and anti-biotin antibody complexes on mobile/fluid SLBs were also rearranged as macrophages engage on opsonized SLBs. Whereas there was no IgG microcluster forming during engagement on immobile/gel-phase SLBs. Such difference in IgG microcluster reorganization affected membrane morphology and spreading area of macrophages during engagement. Macrophages were able to form flower-like morphology on mobile/fluid SLBs, while the membrane was flat on immobile/gel-phase

SLBs. The spreading on mobile/fluid SLBs was larger than that on immobile/gel-phase SLBs. Microclustering events on mobile antigen-antibody complexes enhanced ADCP on Wil2s cells and spreading on SLBs. For successful ADCP, IgG and Syk formed microclusters colocalizing to each other which were propelled-forward with membrane protrusion after aggregation at the base of phagocytic cup. IgG and Syk microclusters were also colocalized during engagement on mobile/fluid SLBs which induced larger spreading compare to immobile/gel-phase SLBs. This suggests that microclustering could aid phagocytic responses by triggering stronger FcγR signals which could explain why the lack of microclustering suppressed phagocytic responses.

The membrane topography of macrophages while engaging on mobile/fluid and immobile/gel-phase SLBs was also investigated by using pol-TIRF imaging. It was noticeable that podosome-like structures and the leading edge were formed around IgG miroclusters where the membrane was relatively flat. However, membrane surrounding podosome-like structures was relatively perpendicular. This topography implies that there should be pulling forces around podosome-like structure which could be related to the trogocytic biting on opsonized Wil2s cells. Trogocytosis occurred on Wil2s cells when IgG microclusters colocalizing with Syk were concentrated at the base of phagocytic cup. This suggested the importance of proper distribution of FcγR signaling around phagocytic cup for successful ADCP while suppressing trogocytosis. Trogocytosis was also triggered while CK 666 treated macrophages engaging on WIL2-S cells. Syk KO macrophages could form microclusters, but they only triggered trogocytosis. This data strengthens the importance of Syk and Arp2/3 activity to successfully engulf the target while suppressing trogocytosis. During engagement on mobile/fluid SLBs, IgG microclusters were

colocalized with Syk and Akt PH which were propelled forward with the leading edge or left behind forming podosome-like structures. However, macrophages could not engage properly on SLBs after CK 666 treatment or without Syk while IgG microclusters were still formed.

All these data suggest that Syk mediated actin branching and nucleation via PI3K and Arp2/3 activity contributes significantly for ADCP. From our finding, we speculate that FcγR microclustering during ADCP is driven by changes in the actin cytoskeleton and possibly by transmembrane proteins bound to actin. Transmembrane proteins affecting FcγR microclustering could include CD44 that directly binds to the actin cytoskeleton via ezrin (Niedergang & Grinstein, 2018; Ostrowski, Grinstein, & Freeman, 2016). CD45 could also be connected to actin via ankyrin which regulates FcγR microclustering (Hashimoto-Tane & Saito, 2016; Ostrowski et al., 2016). These transmembrane proteins act as fence at the actin-rich region that inhibit FcγR lateral diffusion. During engagement on IgG-coated coverslips, FcγRs in the actin-rich area were more confined, while the leading edge had more freely moving FcγRs; However, Syk activity is required to increase lateral mobility of FcγRs by reorganizing actin cytoskeleton (Jaumouille et al., 2014). Also, FcγR mobility at the leading edge of migrating macrophages was greater than in the trailing uropod (Freeman et al., 2018). Overall, FcγRs are confined by actin-bound transmembrane proteins before ligation with IgG. Ligation between FcγRs and IgG triggers recruitment of Syk which activate major regulators of the actin cytoskeleton including PI3K, Vav, phospholipase C and Arp2/3. Accordingly, actin reorganization results in increased mobility of FcγR and actin-bound

transmembrane proteins which induces FcγR microclustering. Therefore, activating signal is triggered from FcγR microclusters (Figure 3.1).

Additionally, FcγRs microclustering during phagocytic process have similarities with TCR and BCR microclustering at the immunological synapse. For instance, TCR

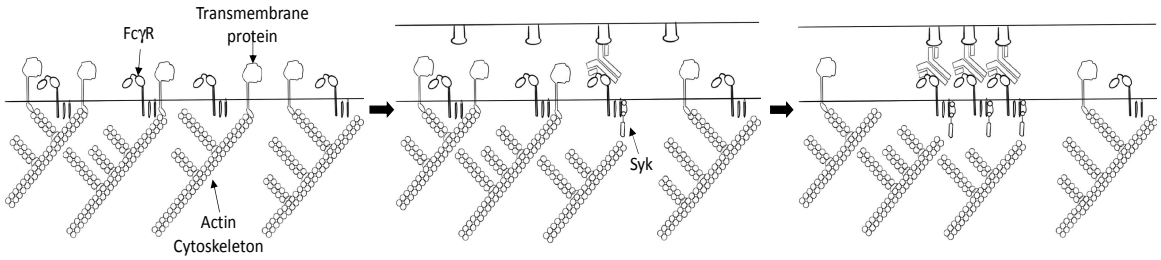

Figure 3.1 FcγR microclustering controlled by actin via syk signal. A) FcγRs are confined by actin-bound transmembrane proteins in normal state. After FcγRs binding to IgG, Syk recruitment is triggered which triggers the actin cytoskeleton reorganization. Actin reorganization increase the mobility of FcγR and actin-bound transmembrane protein. Therefore, FcγR microclustering is enhanced overall which also amplifies FcγR signaling.

forms microclusters which gets rearranged at the immunological synapse on SLBs or antigen-bearing cells (Beemiller, Jacobelli, & Krummel, 2012; Hashimoto-Tane & Saito, 2016). Microclustering is also important mechanism for B cell receptor activation via signaling molecules including Syk, Vav, and Lyn (Ketchum et al., 2014; J. Li et al., 2018). Moreover, both T cell receptor and B cell receptor microclustering were enhanced on mobile/fluid SLBs which triggered higher signals (Hsu et al., 2012; Ketchum et al., 2014). All these studies suggest the similar trend overall with the findings from this project: Microclustering of FcγR are affected by ligand mobility which is important on amplifying signaling. However, our study found a noticeable difference on FcγR microclusters rearrangement at the immunological synapse compare to TCR and BCR. Successful ADCP requires rearrangement of FcγR microclusters colocalizing after accumulation at the base of phagocytic cup during membrane protrusion (Figure 3.1).

This FcγR microclusters rearrangement event is different with TCR and BCR microclustering at the immunological synapse. Both TCR and BCR microclusters form central supramolecular activation complex (cSMAC). The cSMAC formation process is dependent on actin. TCRs form cSMAC by centripetal actin flow, and actin-driven membrane retraction form BCR cSMAC at the immunological synapse (Bolger-Munro et al., 2019; Fleire et al., 2006; Hammer & Burkhardt, 2013). After forming cSMAC, both TCR and BCR maintain cSMAC structure that triggers activating signals. However, it is clear that all TCR, BCR and FcγR colocalize with Syk and Zap 70 which trigger activating signals (Sloan-Lancaster et al., 1997; Wang et al., 2010; Westbroek & Geahlen, 2017). Also, Arp2/3 plays an important role during TCR, BCR and FcγR microclustering and signaling (Bolger-Munro et al., 2019; Zhang et al., 2017). This suggests that immune receptor microclustering event and immune signaling are dependent on Arp2/3 mediated actin nucleation and polymerization.

Together, there are many similarities among TCR, BCR and FcγR microclustering and signaling. Microclustering of TCR, BCR and FcγRs enhance signal amplification compare to when microclustering was suppressed. For microclustering, Syk and Zap 70 mediated actin reorganization is important (Jaumouille et al., 2014; Sloan-Lancaster et al., 1997; Wang et al., 2010; Westbroek & Geahlen, 2017). Moreover, the ligand mobility affects TCR and BCR microclustering and activation which is similar to the data from our study showed antigen-antibody mobility affecting FcγR microclustering and ADCP. Microclustering of TCR and BCR enhanced signal amplification during engagement on mobile ligands than on immobile ligands (Hsu et al., 2012; Ketchum et al., 2014). However, more research is needed to elucidate how actin regulates microclustering event

that can also be affected by ligand mobility. Also, the reason why only FcγR microclusters are rearranged after accumulation at the base of phagocytic cup while TCR and BCR only form cSMAC is also not known yet. Overall, this dissertation provides a new insight into the importance of antigen-antibody mobility for FcγR microclustering and ADCP.

References

Abram, C. L., & Lowell, C. A. (2017). Shp1 function in myeloid cells. *J Leukoc Biol, 102*(3), 657-675. doi:10.1189/jlb.2MR0317-105R

Ackerman, M. E., Dugast, A. S., McAndrew, E. G., Tsoukas, S., Licht, A. F., Irvine, D. J., & Alter, G. (2013). Enhanced phagocytic activity of HIV-specific antibodies correlates with natural production of immunoglobulins with skewed affinity for FcgammaR2a and FcgammaR2b. *J Virol, 87*(10), 5468-5476. doi:10.1128/JVI.03403-12

Alvey, C., & Discher, D. E. (2017). Engineering macrophages to eat cancer: from "marker of self" CD47 and phagocytosis to differentiation. *J Leukoc Biol, 102*(1), 31-40. doi:10.1189/jlb.4RI1216-516R

Alvey, C. M., Spinler, K. R., Irianto, J., Pfeifer, C. R., Hayes, B., Xia, Y., . . . Discher, D. E. (2017). SIRPA-Inhibited, Marrow-Derived Macrophages Engorge, Accumulate, and Differentiate in Antibody-Targeted Regression of Solid Tumors. *Curr Biol, 27*(14), 2065-2077 e2066. doi:10.1016/j.cub.2017.06.005

Bailey, E. M., Choudhury, A., Vuppula, H., Ortiz, D., Schaeck, J., Manning, A. M., . . . Hoppe, A. D. (2020). Engineered IgG1-Fc molecules define valency control of cell surface Fcg receptor inhibition and activation in endosomes. doi:10.3389/fimmu.2020.617767

Bakalar, M. H., Joffe, A. M., Schmid, E. M., Son, S., Podolski, M., & Fletcher, D. A. (2018). Size-Dependent Segregation Controls Macrophage Phagocytosis of Antibody-Opsonized Targets. *Cell, 174*(1), 131-142 e113. doi:10.1016/j.cell.2018.05.059

Barkal, A. A., Weiskopf, K., Kao, K. S., Gordon, S. R., Rosental, B., Yiu, Y. Y., . . . Maute, R. L. (2018). Engagement of MHC class I by the inhibitory receptor LILRB1 suppresses macrophages and is a target of cancer immunotherapy. *Nat Immunol, 19*(1), 76-84. doi:10.1038/s41590-017-0004-z

Beemiller, P., Jacobelli, J., & Krummel, M. F. (2012). Integration of the movement of signaling microclusters with cellular motility in immunological synapses. *Nat Immunol, 13*(8), 787-795. doi:10.1038/ni.2364

Bolger-Munro, M., Choi, K., Scurll, J. M., Abraham, L., Chappell, R. S., Sheen, D., . . . Gold, M. R. (2019). Arp2/3 complex-driven spatial patterning of the BCR enhances immune synapse formation, BCR signaling and B cell activation. *Elife, 8*. doi:10.7554/eLife.44574

Boross, P., Jansen, J. H., de Haij, S., Beurskens, F. J., van der Poel, C. E., Bevaart, L., . . . Leusen, J. H. (2011). The in vivo mechanism of action of CD20 monoclonal antibodies depends on local tumor burden. *Haematologica, 96*(12), 1822-1830. doi:10.3324/haematol.2011.047159

Boudreau, C. M., & Alter, G. (2019). Extra-Neutralizing FcR-Mediated Antibody Functions for a Universal Influenza Vaccine. *Front Immunol, 10*, 440. doi:10.3389/fimmu.2019.00440

Brandsma, A. M., Hogarth, P. M., Nimmerjahn, F., & Leusen, J. H. (2016). Clarifying the Confusion between Cytokine and Fc Receptor "Common Gamma Chain". *Immunity, 45*(2), 225-226. doi:10.1016/j.immuni.2016.07.006

Brandsma, A. M., Schwartz, S. L., Wester, M. J., Valley, C. C., Blezer, G. L. A., Vidarsson, G., . . . Leusen, J. H. W. (2018). Mechanisms of inside-out signaling of the high-affinity IgG receptor FcgammaRI. *Sci Signal, 11*(540). doi:10.1126/scisignal.aaq0891

Breitsprecher, D., & Goode, B. L. (2013). Formins at a glance. *J Cell Sci, 126*(Pt 1), 1-7. doi:10.1242/jcs.107250

Burtnick, L. D., Koepf, E. K., Grimes, J., Jones, E. Y., Stuart, D. I., McLaughlin, P. J., & Robinson, R. C. (1997). The crystal structure of plasma gelsolin: implications for actin severing, capping, and nucleation. *Cell, 90*(4), 661-670. doi:10.1016/s0092-8674(00)80527-9

Chao, M. P., Alizadeh, A. A., Tang, C., Myklebust, J. H., Varghese, B., Gill, S., . . . Majeti, R. (2010). Anti-CD47 antibody synergizes with rituximab to promote phagocytosis and eradicate non-Hodgkin lymphoma. *Cell, 142*(5), 699-713. doi:10.1016/j.cell.2010.07.044

Chen, B., Chou, H. T., Brautigam, C. A., Xing, W., Yang, S., Henry, L., . . . Rosen, M. K. (2017). Rac1 GTPase activates the WAVE regulatory complex through two distinct binding sites. *Elife, 6*. doi:10.7554/eLife.29795

Chen, B. C., Legant, W. R., Wang, K., Shao, L., Milkie, D. E., Davidson, M. W., . . . Betzig, E. (2014). Lattice light-sheet microscopy: imaging molecules to embryos at high spatiotemporal resolution. *Science, 346*(6208), 1257998. doi:10.1126/science.1257998

Church, A. K., VanDerMeid, K. R., Baig, N. A., Baran, A. M., Witzig, T. E., Nowakowski, G. S., & Zent, C. S. (2016). Anti-CD20 monoclonal antibody-dependent phagocytosis of chronic lymphocytic leukaemia cells by autologous macrophages. *Clin Exp Immunol, 183*(1), 90-101. doi:10.1111/cei.12697

Dahal, L. N., Dou, L., Hussain, K., Liu, R., Earley, A., Cox, K. L., . . . Beers, S. A. (2017). STING Activation Reverses Lymphoma-Mediated Resistance to Antibody Immunotherapy. *Cancer Res, 77*(13), 3619-3631. doi:10.1158/0008-5472.CAN-16-2784

Dahal, L. N., Huang, C. Y., Stopforth, R. J., Mead, A., Chan, K., Bowater, J. X., . . . Beers, S. A. (2018). Shaving Is an Epiphenomenon of Type I and II Anti-CD20-Mediated Phagocytosis, whereas Antigenic Modulation Limits Type I Monoclonal Antibody Efficacy. *J Immunol, 201*(4), 1211-1221. doi:10.4049/jimmunol.1701122

Dominguez, R., & Holmes, K. C. (2011). Actin structure and function. *Annu Rev Biophys, 40*, 169-186. doi:10.1146/annurev-biophys-042910-155359

Eden, S., Rohatgi, R., Podtelejnikov, A. V., Mann, M., & Kirschner, M. W. (2002). Mechanism of regulation of WAVE1-induced actin nucleation by Rac1 and Nck. *Nature, 418*(6899), 790-793. doi:10.1038/nature00859

Egile, C., Rouiller, I., Xu, X. P., Volkmann, N., Li, R., & Hanein, D. (2005). Mechanism of filament nucleation and branch stability revealed by the structure of the Arp2/3 complex at actin branch junctions. *PLoS Biol, 3*(11), e383. doi:10.1371/journal.pbio.0030383

Fleire, S. J., Goldman, J. P., Carrasco, Y. R., Weber, M., Bray, D., & Batista, F. D. (2006). B cell ligand discrimination through a spreading and contraction response. *Science, 312*(5774), 738-741. doi:10.1126/science.1123940

Fletcher, D. A., & Mullins, R. D. (2010). Cell mechanics and the cytoskeleton. *Nature, 463*(7280), 485-492. doi:10.1038/nature08908

Frank, M., Egile, C., Dyachok, J., Djakovic, S., Nolasco, M., Li, R., & Smith, L. G. (2004). Activation of Arp2/3 complex-dependent actin polymerization by plant proteins distantly related to Scar/WAVE. *Proc Natl Acad Sci U S A, 101*(46), 16379-16384. doi:10.1073/pnas.0407392101

Freeman, S. A., Vega, A., Riedl, M., Collins, R. F., Ostrowski, P. P., Woods, E. C., . . . Grinstein, S. (2018). Transmembrane Pickets Connect Cyto- and Pericellular Skeletons Forming Barriers to Receptor Engagement. *Cell, 172*(1-2), 305-317 e310. doi:10.1016/j.cell.2017.12.023

Goley, E. D., Rammohan, A., Znameroski, E. A., Firat-Karalar, E. N., Sept, D., & Welch, M. D. (2010). An actin-filament-binding interface on the Arp2/3 complex is critical for nucleation and branch stability. *Proc Natl Acad Sci U S A, 107*(18), 8159-8164. doi:10.1073/pnas.0911668107

Goodridge, H. S., Reyes, C. N., Becker, C. A., Katsumoto, T. R., Ma, J., Wolf, A. J., . . . Underhill, D. M. (2011). Activation of the innate immune receptor Dectin-1 upon formation of a 'phagocytic synapse'. *Nature, 472*(7344), 471-475. doi:10.1038/nature10071

Gordan, S., Biburger, M., & Nimmerjahn, F. (2015). bIgG time for large eaters: monocytes and macrophages as effector and target cells of antibody-mediated immune activation and repression. *Immunol Rev, 268*(1), 52-65. doi:10.1111/imr.12347

Gordon, S. R., Maute, R. L., Dulken, B. W., Hutter, G., George, B. M., McCracken, M. N., . . . Weissman, I. L. (2017). PD-1 expression by tumour-associated macrophages inhibits phagocytosis and tumour immunity. *Nature, 545*(7655), 495-499. doi:10.1038/nature22396

Grakoui, A., Bromley, S. K., Sumen, C., Davis, M. M., Shaw, A. S., Allen, P. M., & Dustin, M. L. (1999). The immunological synapse: a molecular machine controlling T cell activation. *Science, 285*(5425), 221-227. doi:10.1126/science.285.5425.221

Griffin, F. M., Jr., Griffin, J. A., Leider, J. E., & Silverstein, S. C. (1975). Studies on the mechanism of phagocytosis. I. Requirements for circumferential attachment of particle-bound ligands to specific receptors on the macrophage plasma membrane. *J Exp Med, 142*(5), 1263-1282. doi:10.1084/jem.142.5.1263

Griffin, F. M., Jr., Griffin, J. A., & Silverstein, S. C. (1976). Studies on the mechanism of phagocytosis. II. The interaction of macrophages with anti-immunoglobulin IgG-coated bone marrow-derived lymphocytes. *J Exp Med, 144*(3), 788-809. doi:10.1084/jem.144.3.788

Guillen, N. (2014). Infection biology: Nibbled to death. *Nature, 508*(7497), 462-463. doi:10.1038/nature13223

Gul, N., & van Egmond, M. (2015). Antibody-Dependent Phagocytosis of Tumor Cells by Macrophages: A Potent Effector Mechanism of Monoclonal Antibody Therapy of Cancer. *Cancer Res, 75*(23), 5008-5013. doi:10.1158/0008-5472.CAN-15-1330

Hammer, J. A., 3rd, & Burkhardt, J. K. (2013). Controversy and consensus regarding myosin II function at the immunological synapse. *Curr Opin Immunol, 25*(3), 300-306. doi:10.1016/j.coi.2013.03.010

Hashimoto-Tane, A., & Saito, T. (2016). Dynamic Regulation of TCR-Microclusters and the Microsynapse for T Cell Activation. *Front Immunol, 7*, 255. doi:10.3389/fimmu.2016.00255

He, W., Chen, C. J., Mullarkey, C. E., Hamilton, J. R., Wong, C. K., Leon, P. E., . . . Tan, G. S. (2017). Alveolar macrophages are critical for broadly-reactive antibody-mediated protection against influenza A virus in mice. *Nat Commun, 8*(1), 846. doi:10.1038/s41467-017-00928-3

Holowka, D., Sil, D., Torigoe, C., & Baird, B. (2007). Insights into immunoglobulin E receptor signaling from structurally defined ligands. *Immunol Rev, 217*, 269-279. doi:10.1111/j.1600-065X.2007.00517.x

Hsu, C. J., Hsieh, W. T., Waldman, A., Clarke, F., Huseby, E. S., Burkhardt, J. K., & Baumgart, T. (2012). Ligand mobility modulates immunological synapse formation and T cell activation. *PLoS One, 7*(2), e32398. doi:10.1371/journal.pone.0032398

Jaumouille, V., Farkash, Y., Jaqaman, K., Das, R., Lowell, C. A., & Grinstein, S. (2014). Actin cytoskeleton reorganization by Syk regulates Fcgamma receptor responsiveness by increasing its lateral mobility and clustering. *Dev Cell, 29*(5), 534-546. doi:10.1016/j.devcel.2014.04.031

Ketchum, C., Miller, H., Song, W., & Upadhyaya, A. (2014). Ligand mobility regulates B cell receptor clustering and signaling activation. *Biophys J, 106*(1), 26-36. doi:10.1016/j.bpj.2013.10.043

Kheir, W. A., Gevrey, J. C., Yamaguchi, H., Isaac, B., & Cox, D. (2005). A WAVE2-Abi1 complex mediates CSF-1-induced F-actin-rich membrane protrusions and migration in macrophages. *J Cell Sci, 118*(Pt 22), 5369-5379. doi:10.1242/jcs.02638

Kim, A. S., Kakalis, L. T., Abdul-Manan, N., Liu, G. A., & Rosen, M. K. (2000). Autoinhibition and activation mechanisms of the Wiskott-Aldrich syndrome protein. *Nature, 404*(6774), 151-158. doi:10.1038/35004513

Kotila, T., Wioland, H., Enkavi, G., Kogan, K., Vattulainen, I., Jegou, A., . . . Lappalainen, P. (2019). Mechanism of synergistic actin filament pointed end depolymerization by cyclase-associated protein and cofilin. *Nat Commun, 10*(1), 5320. doi:10.1038/s41467-019-13213-2

Lambert, T., & Shao, L. (2019). tlambert03/LLSpy: v0.4.8. doi:http://doi.org/10.5281/zenodo.3554482

Li, J., Yin, W., Jing, Y., Kang, D., Yang, L., Cheng, J., . . . Liu, C. (2018). The Coordination Between B Cell Receptor Signaling and the Actin Cytoskeleton During B Cell Activation. *Front Immunol, 9*, 3096. doi:10.3389/fimmu.2018.03096

Li, X., & Kimberly, R. P. (2014). Targeting the Fc receptor in autoimmune disease. *Expert Opin Ther Targets, 18*(3), 335-350. doi:10.1517/14728222.2014.877891

Lin, J., Kurilova, S., Scott, B. L., Bosworth, E., Iverson, B. E., Bailey, E. M., & Hoppe, A. D. (2016). TIRF imaging of Fc gamma receptor microclusters dynamics and signaling on macrophages during frustrated phagocytosis. *BMC Immunol, 17*, 5. doi:10.1186/s12865-016-0143-2

Lin, K. B., Freeman, S. A., Zabetian, S., Brugger, H., Weber, M., Lei, V., . . . Gold, M. R. (2008). The rap GTPases regulate B cell morphology, immune-synapse

formation, and signaling by particulate B cell receptor ligands. *Immunity, 28*(1), 75-87. doi:10.1016/j.immuni.2007.11.019

Linder, S., & Wiesner, C. (2015). Tools of the trade: podosomes as multipurpose organelles of monocytic cells. *Cell Mol Life Sci, 72*(1), 121-135. doi:10.1007/s00018-014-1731-z

Liu, C., Bai, X., Wu, J., Sharma, S., Upadhyaya, A., Dahlberg, C. I., . . . Song, W. (2013). N-wasp is essential for the negative regulation of B cell receptor signaling. *PLoS Biol, 11*(11), e1001704. doi:10.1371/journal.pbio.1001704

Lou, J., Low-Nam, S. T., Kerkvliet, J. G., & Hoppe, A. D. (2014). Delivery of CSF-1R to the lumen of macropinosomes promotes its destruction in macrophages. *J Cell Sci, 127*(Pt 24), 5228-5239. doi:10.1242/jcs.154393

Lowell, C. A. (2011). Src-family and Syk kinases in activating and inhibitory pathways in innate immune cells: signaling cross talk. *Cold Spring Harb Perspect Biol, 3*(3). doi:10.1101/cshperspect.a002352

Machesky, L. M., Mullins, R. D., Higgs, H. N., Kaiser, D. A., Blanchoin, L., May, R. C., . . . Pollard, T. D. (1999). Scar, a WASp-related protein, activates nucleation of actin filaments by the Arp2/3 complex. *Proc Natl Acad Sci U S A, 96*(7), 3739-3744. doi:10.1073/pnas.96.7.3739

Marshall, M. J. E., Stopforth, R. J., & Cragg, M. S. (2017). Therapeutic Antibodies: What Have We Learnt from Targeting CD20 and Where Are We Going? *Front Immunol, 8*, 1245. doi:10.3389/fimmu.2017.01245

Matlung, H. L., Babes, L., Zhao, X. W., van Houdt, M., Treffers, L. W., van Rees, D. J., . . . van den Berg, T. K. (2018). Neutrophils Kill Antibody-Opsonized Cancer Cells by Trogoptosis. *Cell Rep, 23*(13), 3946-3959 e3946. doi:10.1016/j.celrep.2018.05.082

McQuin, C., Goodman, A., Chernyshev, V., Kamentsky, L., Cimini, B. A., Karhohs, K. W., . . . Carpenter, A. E. (2018). CellProfiler 3.0: Next-generation image processing for biology. *PLoS Biol, 16*(7), e2005970. doi:10.1371/journal.pbio.2005970

Millard, T. H., Sharp, S. J., & Machesky, L. M. (2004). Signalling to actin assembly via the WASP (Wiskott-Aldrich syndrome protein)-family proteins and the Arp2/3 complex. *Biochem J, 380*(Pt 1), 1-17. doi:10.1042/BJ20040176

Minard-Colin, V., Xiu, Y., Poe, J. C., Horikawa, M., Magro, C. M., Hamaguchi, Y., . . . Tedder, T. F. (2008). Lymphoma depletion during CD20 immunotherapy in mice is mediated by macrophage FcgammaRI, FcgammaRIII, and FcgammaRIV. *Blood, 112*(4), 1205-1213. doi:10.1182/blood-2008-01-135160

Mocsai, A., Ruland, J., & Tybulewicz, V. L. (2010). The SYK tyrosine kinase: a crucial player in diverse biological functions. *Nat Rev Immunol, 10*(6), 387-402. doi:10.1038/nri2765

Morrissey, M. A., Williamson, A. P., Steinbach, A. M., Roberts, E. W., Kern, N., Headley, M. B., & Vale, R. D. (2018). Chimeric antigen receptors that trigger phagocytosis. *Elife, 7*. doi:10.7554/eLife.36688

Mullarkey, C. E., Bailey, M. J., Golubeva, D. A., Tan, G. S., Nachbagauer, R., He, W., . . . Palese, P. (2016). Broadly Neutralizing Hemagglutinin Stalk-Specific Antibodies Induce Potent Phagocytosis of Immune Complexes by Neutrophils in an Fc-Dependent Manner. *mBio, 7*(5). doi:10.1128/mBio.01624-16

Mullins, R. D., Heuser, J. A., & Pollard, T. D. (1998). The interaction of Arp2/3 complex with actin: nucleation, high affinity pointed end capping, and formation of branching networks of filaments. *Proc Natl Acad Sci U S A, 95*(11), 6181-6186. doi:10.1073/pnas.95.11.6181

Niedergang, F., & Grinstein, S. (2018). How to build a phagosome: new concepts for an old process. *Curr Opin Cell Biol, 50*, 57-63. doi:10.1016/j.ceb.2018.01.009

Nimmerjahn, F., & Ravetch, J. V. (2008). Fcgamma receptors as regulators of immune responses. *Nat Rev Immunol, 8*(1), 34-47. doi:10.1038/nri2206

Ostrowski, P. P., Grinstein, S., & Freeman, S. A. (2016). Diffusion Barriers, Mechanical Forces, and the Biophysics of Phagocytosis. *Dev Cell, 38*(2), 135-146. doi:10.1016/j.devcel.2016.06.023

Pantaloni, D., Boujemaa, R., Didry, D., Gounon, P., & Carlier, M. F. (2000). The Arp2/3 complex branches filament barbed ends: functional antagonism with capping proteins. *Nat Cell Biol, 2*(7), 385-391. doi:10.1038/35017011

Park, H., Chan, M. M., & Iritani, B. M. (2010). Hem-1: putting the "WAVE" into actin polymerization during an immune response. *FEBS Lett, 584*(24), 4923-4932. doi:10.1016/j.febslet.2010.10.018

Pham, T., Mero, P., & Booth, J. W. (2011). Dynamics of macrophage trogocytosis of rituximab-coated B cells. *PLoS One, 6*(1), e14498. doi:10.1371/journal.pone.0014498

Planchon, T. A., Gao, L., Milkie, D. E., Davidson, M. W., Galbraith, J. A., Galbraith, C. G., & Betzig, E. (2011). Rapid three-dimensional isotropic imaging of living cells using Bessel beam plane illumination. *Nat Methods, 8*(5), 417-423. doi:10.1038/nmeth.1586

Pollard, T. D., & Borisy, G. G. (2003). Cellular motility driven by assembly and disassembly of actin filaments. *Cell, 112*(4), 453-465. doi:10.1016/s0092-8674(03)00120-x

Pollitt, A. Y., & Insall, R. H. (2009). WASP and SCAR/WAVE proteins: the drivers of actin assembly. *J Cell Sci, 122*(Pt 15), 2575-2578. doi:10.1242/jcs.023879

Quinn, S. E., Huang, L., Kerkvliet, J. G., Swanson, J. A., Smith, S., Hoppe, A. D., . . . Scott, B. L. (2020). The structural dynamics of macropinosome formation and PI3-kinase-mediated sealing revealed by lattice light sheet microscopy. *BioRxiv*, 2020.2012.2001.390195. doi:10.1101/2020.12.01.390195

Rey-Suarez, I., Wheatley, B. A., Koo, P., Bhanja, A., Shu, Z., Mochrie, S., . . . Upadhyaya, A. (2020). WASP family proteins regulate the mobility of the B cell receptor during signaling activation. *Nat Commun, 11*(1), 439. doi:10.1038/s41467-020-14335-8

Rotty, J. D., Wu, C., & Bear, J. E. (2013). New insights into the regulation and cellular functions of the ARP2/3 complex. *Nat Rev Mol Cell Biol, 14*(1), 7-12. doi:10.1038/nrm3492

Schindelin, J., Arganda-Carreras, I., Frise, E., Kaynig, V., Longair, M., Pietzsch, T., . . . Cardona, A. (2012). Fiji: an open-source platform for biological-image analysis. *Nat Methods, 9*(7), 676-682. doi:10.1038/nmeth.2019

Scott, B. L., Sochacki, K. A., Low-Nam, S. T., Bailey, E. M., Luu, Q., Hor, A., . . . Hoppe, A. D. (2018). Membrane bending occurs at all stages of clathrin-coat

assembly and defines endocytic dynamics. *Nature Communications, 9*. doi:ARTN 419
10.1038/s41467-018-02818-8

Shapouri-Moghaddam, A., Mohammadian, S., Vazini, H., Taghadosi, M., Esmaeili, S. A., Mardani, F., . . . Sahebkar, A. (2018). Macrophage plasticity, polarization, and function in health and disease. *J Cell Physiol, 233*(9), 6425-6440. doi:10.1002/jcp.26429

Sips, M., Krykbaeva, M., Diefenbach, T. J., Ghebremichael, M., Bowman, B. A., Dugast, A. S., . . . Alter, G. (2016). Fc receptor-mediated phagocytosis in tissues as a potent mechanism for preventive and therapeutic HIV vaccine strategies. *Mucosal Immunol, 9*(6), 1584-1595. doi:10.1038/mi.2016.12

Sloan-Lancaster, J., Zhang, W., Presley, J., Williams, B. L., Abraham, R. T., Lippincott-Schwartz, J., & Samelson, L. E. (1997). Regulation of ZAP-70 intracellular localization: visualization with the green fluorescent protein. *J Exp Med, 186*(10), 1713-1724. doi:10.1084/jem.186.10.1713

Sobota, A., Strzelecka-Kiliszek, A., Gladkowska, E., Yoshida, K., Mrozinska, K., & Kwiatkowska, K. (2005). Binding of IgG-opsonized particles to Fc gamma R is an active stage of phagocytosis that involves receptor clustering and phosphorylation. *J Immunol, 175*(7), 4450-4457. doi:10.4049/jimmunol.175.7.4450

Stanford, S. M., Rapini, N., & Bottini, N. (2012). Regulation of TCR signalling by tyrosine phosphatases: from immune homeostasis to autoimmunity. *Immunology, 137*(1), 1-19. doi:10.1111/j.1365-2567.2012.03591.x

Swanson, J. A., & Hoppe, A. D. (2004). The coordination of signaling during Fc receptor-mediated phagocytosis. *J Leukoc Biol, 76*(6), 1093-1103. doi:10.1189/jlb.0804439

Takenawa, T., & Suetsugu, S. (2007). The WASP-WAVE protein network: connecting the membrane to the cytoskeleton. *Nat Rev Mol Cell Biol, 8*(1), 37-48. doi:10.1038/nrm2069

Tsai, R. K., & Discher, D. E. (2008). Inhibition of "self" engulfment through deactivation of myosin-II at the phagocytic synapse between human cells. *J Cell Biol, 180*(5), 989-1003. doi:10.1083/jcb.200708043

Vaughan, A. T., Chan, C. H., Klein, C., Glennie, M. J., Beers, S. A., & Cragg, M. S. (2015). Activatory and inhibitory Fcgamma receptors augment rituximab-mediated internalization of CD20 independent of signaling via the cytoplasmic domain. *J Biol Chem, 290*(9), 5424-5437. doi:10.1074/jbc.M114.593806

Velmurugan, R., Challa, D. K., Ram, S., Ober, R. J., & Ward, E. S. (2016). Macrophage-Mediated Trogocytosis Leads to Death of Antibody-Opsonized Tumor Cells. *Mol Cancer Ther, 15*(8), 1879-1889. doi:10.1158/1535-7163.MCT-15-0335

Wang, H., Kadlecek, T. A., Au-Yeung, B. B., Goodfellow, H. E., Hsu, L. Y., Freedman, T. S., & Weiss, A. (2010). ZAP-70: an essential kinase in T-cell signaling. *Cold Spring Harb Perspect Biol, 2*(5), a002279. doi:10.1101/cshperspect.a002279

Watrach, A. M., Hanson, L. E., & Watrach, M. A. (1963). The Structure of Infectious Laryngotracheitis Virus. *Virology, 21*, 601-608. doi:10.1016/0042-6822(63)90233-2

Weiskopf, K., & Weissman, I. L. (2015). Macrophages are critical effectors of antibody therapies for cancer. *MAbs, 7*(2), 303-310. doi:10.1080/19420862.2015.1011450

Westbroek, M. L., & Geahlen, R. L. (2017). Modulation of BCR Signaling by the Induced Dimerization of Receptor-Associated SYK. *Antibodies (Basel), 6*(4). doi:10.3390/antib6040023

Woof, J. M., & Burton, D. R. (2004). Human antibody-Fc receptor interactions illuminated by crystal structures. *Nat Rev Immunol, 4*(2), 89-99. doi:10.1038/nri1266

Zhang, Y., Shen, H., Liu, H., Feng, H., Liu, Y., Zhu, X., & Liu, X. (2017). Arp2/3 complex controls T cell homeostasis by maintaining surface TCR levels via regulating TCR(+) endosome trafficking. *Sci Rep, 7*(1), 8952. doi:10.1038/s41598-017-08357-4